Stony Brook University

Lipid Raft and Sterol Interactions of the Beta-Barrel Forming Toxin Perfringolysin O

A Dissertation Presented

by

Lindsay D. Nelson

to

The Graduate School

in Partial Fulfillment of the Requirements

for the Degree of

Doctor of Philosophy

in

Molecular and Cellular Biology

Stony Brook University

August 2009

The Graduate School

Lindsay D. Nelson

We, the dissertation committee for the above candidate for the

Doctor of Philosophy degree, hereby recommend

acceptance of this dissertation.

Dr. Erwin London, Ph.D.– Dissertation Advisor
Professor, Department of Biochemistry and Cell Biology

Dr. Deborah Brown, Ph.D. - Chairperson of Defense
Professor, Department of Biochemistry and Cell Biology

Dr. David Thanassi, Ph.D.
Associate Professor, Department of Molecular Genetics and Microbiology

Dr. James Bliska, Ph.D
Professor, Department of Molecular Genetics and Microbiology

This dissertation is accepted by the Graduate School

Lawrence Martin
Dean of the Graduate School

Abstract of the Dissertation

Lipid Raft and Sterol Interactions of the Beta-Barrel Forming Toxin Perfringolysin O

by

Lindsay D. Nelson

Doctor in Philosophy

in

Molecular and Cellular Biology

Stony Brook University

2009

Lipid rafts are ordered regions of the membrane enriched in cholesterol and saturated lipid. They are believed to co-exist with domains composed of disordered lipids. In order to investigate how transmembrane (TM) proteins can associate with lipid rafts, membrane binding and lipid raft affinity of the sterol-dependent, pore-forming cytolysin perfringolysin O were analyzed using model membranes.

To understand the molecular basis of PFO membrane interaction, its dependence upon sterol structure, lipid structure, and aqueous environment was measured using fluorescence spectroscopy. PFO sterol binding was affected by double bond location of

the sterol rings, sterol side chain structure, and sterol polar group structure. However, a sterol structure promoting formation of ordered domains was not critical for interaction. PFO membrane interaction was also affected by phospholipid acyl chain structure, being inversely related to tight acyl chain packing with cholesterol. Sterol binding strength and specificity was not affected by whether PFO forms a TM beta-barrel. Additional experiments demonstrated that low pH enhanced PFO membrane binding, oligomerization, and pore formation, consistent with the hypothesis that PFO functions in acidic vesicles.

To measure lipid raft affinity of PFO, a novel fluorescence resonance energy transfer (FRET) assay was used. In contrast to an alpha-helical TM peptide, PFO had significant raft affinity, although its affinity was reduced after formation of the TM beta-barrel. Cholesterol binding was found to be required for PFO raft association. However, PFO did not simply follow membrane cholesterol into rafts, because although ceramide displaced cholesterol from ordered domains, it did not displace PFO. The ability of PFO to bind to detergent resistant membranes (DRMs), which are derived from ordered lipid domains, was also studied. In all lipid mixtures examined, PFO was more strongly associated with DRMs than with ordered domains as measured by FRET, suggesting when PFO is bound to a lipid raft, it may actually be more locally associated with disordered lipids. Combined, these studies have suggested a model for PFO raft affinity that is not solely dependent upon cholesterol concentrations within ordered domains, but also upon the ability of the complex of PFO and bound cholesterol to pack favorably into ordered domains.

Dedication

This dissertation is dedicated, with love, in memory of my maternal grandparents Nancy and Robert Leiper, whom I miss everyday.

Table of Contents

Chapter 3: Effect of sterol and lipid structure on PFO membrane interaction

Chapter 4: PFO raft affinity and its dependence on lipid composition

Chapter 5: Summary and Future Directions

List of Abbreviations

PFO	Perfringolysin O
WT	wild-type
MUT	mutant
CT-B	Cholera Toxin B
TM	transmembrane
Trp	tryptophan
FRET	fluorescence resonance energy transfer
DRM	detergent resistant membrane
Lo	liquid ordered
Ld	liquid disordered
SDS-AGE	sodium dodecyl sulfate -agarose gel electrophoresis
SM	sphingomyelin
DOPC	dioleoylphosphatidylcholine
CHOL	cholesterol
CER	ceramide
cer-rich	ceramide rich
DPPC	dipalmitoylphosphatidylcholine
POPC	palmityoyloleoylphosphatidylcholine
DPhPC	diphytanoylphosphatidylcholine
DMoPC	dimyristoleoylphosphatidylcholine
DOPE	dioleoylphosphatidylethanolamine
DSPC	distearoylphosphatidylcholine
LcTMADPH	long chain trimethyl amino diphenylhexatriene

List of Figures

List of Tables

Acknowledgements

First and foremost, I would like to thank my thesis advisor, Dr. Erwin London, for his kindness, patience, and support as he mentored me throughout my time as a graduate student. He has provided me with endless guidance and advice which has been invaluable to both my research and my life. His intelligence, integrity, and his genuine care and concern for not only myself, but for all of his students, makes him not only an exemplary scientist and mentor, but also an outstanding human being.

I would like to sincerely thank my committee members, Dr. Debbie Brown, Dr. David Thanassi, Dr. Jim Bliska, and Dr. Sandy Simon for their helpful suggestions with my thesis project over the past few years, and for their comments which have improved the contents of this dissertation. I would especially like to thank Debbie for agreeing to serve as my chairperson, and for always providing me with timely and thoughtful feedback after my committee meetings.

Many thanks to our collaborator Dr. Art Johnson for helpful discussions over the course of the project, as well as Dr. Alex Heuck for providing me with materials that were necessary to my research.

Thanks to all the past and present London lab members (Gang, Bing, Jie, Megha, Omar, Shyam, Khurshida, Hui-Ting, Mi Jin, and Priya) that have provided me unlimited technical support, and have made working in the lab a pleasure. I especially appreciate Megha and Omar for helping me get acquainted with life in the lab, and for their constant advice and friendship, which I will always cherish.

I also must thank all my friends at Stony Brook. They have made graduate school bearable, and Long Island a place I can call home. I am indebted to my first year MCB classmates (Erin, Jamie, Lisa, Jason, Tim, Malgosia, Grigor, Rahul, Aftab, Nusrat, John, and Mike) who have been like family to me, and have given me memories I will always hold dear to my heart. Thanks to Kate, Kasey, and Beth for reminding me of the simple joys in life: good food and great company. I especially have to give infinite thanks to Erin for being a best friend to me since the very first day I met her.

I must thank my family for always being a source of strength and encouragement to me throughout my journey in graduate school. I thank my sisters Jill, Hayley, Abbey, and Hannah, who always make me laugh even in the most dire of circumstances, which is sometimes when it is most needed. Lastly, I must thank my parents for instilling in me the drive to reach my goals, and for all of their love and support to ensure that I do.

CHAPTER 1
Introduction

The plasma membrane of a eukaryotic cell contains a bilayer of lipids which functions as a selective barrier to tightly regulate transport of materials into and out of the cell. Lipid rafts are believed to be ordered regions of the cell membrane which are composed primarily of sphingolipids with saturated acyl chains and cholesterol, and to co-exist with disordered domains composed primarily of phospholipids with at least one unsaturated acyl chain. Since their proposed existence in cell membranes, lipid rafts have been implicated in important biological processes such as endocytosis, signal transduction, apoptosis and viral/bacterial pathogenesis by serving as platforms to aid in protein-protein interactions on the membrane surface [1-7] .

Defining liquid ordered (Lo) domains (lipid rafts)

Lipid bilayers can exist in three distinct phases (illustrated in Figure 1.1). These phases are dependent upon both temperature and the structure of the lipids in the bilayer. Saturated lipids (lipids that lack double bonds in their acyl chains) can pack together very tightly in the membrane, and at physiologically relevant temperatures, exist in a gel (solid-like) state in which lateral motion is slow . Conversely, unsaturated lipids (which have one or more double bonds in one or both of their acyl chains), form loosely packed bilayers that are in the liquid- disordered (Ld, or fluid) state. Lateral motion in Ld bilayers is very high. The liquid-ordered (Lo) state occurs when saturated lipids are mixed with cholesterol. This phase is unique in that the lipids within Lo bilayers are still packed together very tightly (similar to the gel state), however lateral motion is still very high (similar to the Ld state). At higher temperatures, bilayers in the gel and Lo state will melt into the disordered state. Conversely, at low temperatures, bilayers in the Ld state solidify into the Lo state if there is cholesterol present, or to the gel state if it is not [8-10].

In early model membrane studies, it was demonstrated that making mixed bilayers of both saturated (i.e. sphingolipids) and unsaturated lipids (i.e. phospholipids) resulted in a membrane composed of two distinct co-existing gel and Ld domains [11]. The addition of cholesterol to these bilayers allowed for observance of co-existing Lo domains as well [10]. Co-existing Lo and Ld domains in model membranes have been detected using nuclear magnetic resonance (NMR), fluorescence techniques, and visualized using light microscopy [12-17].

The notion that co-existing domains could function in cells came about initially from the idea that glycosphingolipid-rich regions of polarized epithelial cells (called lipid rafts) might be involved in sorting of apically-directed proteins, including glycosylphophatidylinositol (GPI)-anchored proteins [18, 19]. It was known that certain regions of cellular membranes were resistant to solubilization by the detergent TX-100 at low temperatures [20]. A later study of GPI-anchored proteins showed them to be highly enriched in these detergent-resistant membranes (DRMs) alongside high amounts of sphingolipids and cholesterol [21]. Combined with the knowledge previously afforded by model membrane studies, it was then postulated that DRMs might correspond to regions of the membrane that exist in the Lo state, and thus the hypothesis that lipid rafts were cellular Lo domains was brought forth [22].

DRM studies in model membranes mimicking the lipid composition of the outer leaflet of the plasma membrane (sphingolipids, unsaturated phospholipids, and cholesterol) confirmed that detergent-resistance occurred in such mixtures at physiological temperatures, and only when pre-existing Lo domains were present as measured by fluorescence quenching [23, 24]. This correlation of DRMs to lipid rafts, along with visualization of lipid rafts using other methods, has helped the scientific

community accept the existence of lipid rafts in model membranes [25]. However, in cells the story has turned out not to be so clear (as discussed in future sections) so currently the existence of lipid rafts in cells still remains controversial.

Studying lipid rafts in model membranes

Our lab is interested in defining key principles which affect membrane organization in model membranes, in order to understand the biological implications of lipid rafts in cells. Model membranes are an amazing system to study lipid rafts because their lipid composition can be controlled. This provides the ability to measure how different lipids affect ordered domain formation.

Fluorescence spectroscopic techniques can be used to measure ordered domain formation in model membranes (reviewed in [26-28]). The probes used in membrane studies either have fluorescent properties which are dependent upon membrane fluidity, or they have a preferential affinity for Ld or Lo domains. Short-range quenching and fluorescent resonance energy transfer (FRET) are used to detect partitioning of probes between Lo and Ld domains [24, 29, 30]. Probes which partition into Ld domains will be quenched more by FRET acceptors that partition in Ld domains, and less by FRET acceptors that partition into Lo domains. Confocal microscopy of giant unilamellar vesicles (GUVs) is also frequently used with fluorescently labeled lipid probes which have Ld affinity [13, 14, 16, 31, 32].

Using model membranes, it has been shown how lipid structure affects ordered domain formation. Lipid acyl chain length and saturation are important, as long, saturated acyl chains pack more tightly in the membrane and ordered domains form more easily in these lipid mixtures than in mixtures composed of short, unsaturated acyl chains

[33] . Large polar headgroups on phospholipids tend to inhibit tight packing, and thus inhibit domain formation [33] . Also, it should be noted that ability of some lipids to mix poorly actually promotes the formation of ordered domains in model membranes [34]. Because cholesterol is a crucial component of Lo domains, the ability of other sterols to promote ordered domain formation has been examined [35-38]. Ceramide, a sphingolipid present in cells, has a small polar headgroup similar to cholesterol. The "umbrella model" postulates that the headgroups of phospholipids and sphingolipids act like umbrellas, limiting the exposure of the hydrophobic portions of cholesterol to water (cholesterol having too small a polar headgroup to fully shield itself from aqueous solution) [39]. Since ceramide and cholesterol both have a small polar headgroups, it is believed they compete for the space underneath phospholipid headgroups. Because of this, ceramide displaces cholesterol from Lo domains, forming ceramide-rich domains whose properties are more gel-like than Lo-like [40-43]. Also, the presence of ceramide has been shown to cause rearrangement of lipids, converting nanodomains into large domains visible by microscopy [44, 45].

There are several reasons why model membranes studies are not always perfect. One is that the exact lipid composition of the eukaryotic plasma membrane is still not known. This makes mimicking cellular membranes difficult. It is probable, however, that cholesterol concentration in cells is very high. It has been shown in model membranes that as cholesterol concentration increases, domain size decreases [46]. This may mean that Lo domains in cells actually have nanometer dimensions, which would explain why lipid rafts are unable to be visualized using light microscopy in cells (at least without the addition of external agents), but can be measured using FRET [47]. Also, the plasma membrane is asymmetric (illustrated in Figure 1.2). In mammalian cells, sphingolipids and cholesterol are enriched in the outer leaflet but the inner leaflet is

composed primarily of unsaturated phosphatidylserines (PS) and phosphatidylethanolamines (PE). It is unclear if lipid rafts can form in the inner leaflet, although recent studies have shown that raft formation in the outer SM-rich leaflet can induce raft formation in the inner leaflet [48, 49]. Several researchers have tried to address this problem by developing methods to create asymmetric model membranes (planar bilayers or vesicles) to more closely mimic cellular plasma membranes [50, 51]. Finally, most model membrane studies examine lipid-lipid interactions. However, the plasma membrane of eukaryotic cells contains high concentrations of proteins. It is currently believed that protein-lipid interactions and protein-protein interactions might actually be the driving forces of lipid raft formation in cells (see below).

Cellular studies of lipid rafts

One current model for lipid rafts in cells is that they are most likely small, nanoscopic domains, which, upon addition of key proteins which bind to raft lipid components, trigger clustering of these small ordered domains into large microscopic rafts which in turn triggers cellular events. A notable example of a raft binding protein is cholera toxin (CT), part of the family of AB_5 toxins. Each one of its five B subunits binds to, and clusters the raft lipid ganglioside GM1 on the surface of the host cell. Clustering triggers endocytosis which allows its traffic from the plasma membrane to the golgi to the ER, where it retro-translocates into the host cytosol [52-54], reviewed in [55, 56].

The methods used to study lipid rafts in cells are not perfect. Since it was shown that DRMs might correlate to regions of the cell membrane that are in the Lo state, many studies began to characterize the proteins and lipids that were enriched in DRMs to correlate lipid rafts with their biological function in cells, thus equating lipid rafts with

essential physiological functions. There are some caveats associated with doing so (reviewed in [57-59]). Briefly, many proteins which are found predominately in DRMs are actually uniformly distributed throughout the membrane when measured by fluorescence methods such as FRET [60-63]. This may be because DRMs can only be isolated from cells at 4 degrees, not at physiological temperatures [64]. Since phase behavior of membranes is highly temperature dependent, cooling cells before detergent treatment might exaggerate the amount of Lo domains present at physiological temperatures. Because of this, proteins found to be associated with DRMs might have an affinity for ordered domains, but may not be found in lipid rafts under physiologically relevant conditions. The majority of cellular lipid raft studies now include microscopy techniques, alongside DRM analysis, to confirm protein-lipid raft association.

How do transmembrane proteins associate with lipid rafts?

Many cellular studies have implicated lipid rafts in a variety of biological processes due to the proteins which seem to localize to lipid rafts in cell membranes. The nature of how peripheral proteins (i.e. cholera toxin) can interact with lipid rafts is understood, because these proteins bind to membrane components (saturated lipids) or have lipid modifications whose structure permits them to be associated with lipids rafts. Transmembrane (TM) proteins, on the other hand, have hydrophobic segments which insert into the membrane. These segments are rigid and their surfaces would not seem to permit them to pack well with lipids in the ordered state. Studies with an TM alpha-helical peptide have confirmed this [65].

This question is confounded by the fact that TM sequences found to be associated with rafts in cells do not show ordered domain affinity in model membranes. This is the case for the linker for activation of T-cells (LAT). Upon stimulation, T-cell receptors

(TCR) causes aggregation of lipid rafts, which recruits downstream activators of the signally cascade (e.g. LAT) (recently reviewed in [66, 67]). LAT protein is palmitoylated and is also found in DRMs in cells. When DRM studies using only the palmitoylated portion of LAT are performed in model membranes, LAT peptide is not found in ordered domains to the same extent as the full length LAT protein is in cells [68]. This suggests that TM proteins have other factors besides their sequence and structure to hold them in ordered domains.

Some TM proteins that are targeted to lipid rafts in cells bind to lipids which have an association for ordered domains, such as gangliosides or cholesterol. It is believed this TM protein-lipid association helps hold TM proteins in rafts. A large class of TM beta-barrel forming proteins, the cholesterol dependent cytolysins (CDCs) are the most notable example of this type of protein.

Beta-barrel forming toxins

Beta-barrel forming toxins (BBFTs) are a large, structurally diverse superfamily of proteins which form pores in cell membranes. Most notably they are found in both gram-positive and gram-negative bacteria to aid in pathogenesis [69, 70], but are also present in human immune cells to aid in apoptosis [71]. BBFTs all exist as water soluble monomers which later form TM pores.

Cholesterol dependent cytolysins (CDCs) are a subset of BBFTs which are secreted (in almost all cases) by 20 species from the genera Clostridium, Listeria, Arcanobacterium, Streptococcus, and Bacillus (reviewed in [72]). As their name implies, they all require membrane cholesterol to form pores, and all but two known CDCs also require cholesterol for initial binding to membranes [73, 74].

The structure of perfringolysin O (PFO), the first CDC to have its structure solved [75], is shown in Figure 1.3. It is composed of an N-terminal region which is involved in membrane insertion (domains 1-3), and a C-terminal domain (domain 4) involved in membrane cholesterol recognition. After PFO binds to membrane cholesterol as a monomer, oligomerization occurs on the cell surface forming what is referred to as a "pre-pore" structure which has been estimated to involve between 20 and 50 monomers [73]. Once oligomerization is complete, TM insertion is triggered. This process is illustrated in Figure 1.4. It is believed that structural changes that occur within the C-terminal membrane binding domain trigger conformational changes within the N-terminal region, which allow for formation of the TM structure [76, 77]. Within each monomer, insertion requires two clusters of alpha-helices within the N-terminal region (domain 3) to convert to four beta-strands, while a significant vertical collapse occurs within the N-terminal region (domain 2) to bring these strands close to the membrane surface [78]. The resulting pore is up to 300 angstroms in size, and is lined with a beta-barrel [73].

How exactly CDCs interact with cholesterol is still not completely known. The bulk of our understanding of CDC-cholesterol interactions come from comparative studies between CDCs that require cholesterol for membrane binding (PFO) and one that does not (intermedilysin ILY) [79, 80]. ILY specifically recognizes the glycoprotein CD59, human receptor for complement [74]. It differs in its sequence from PFO in a region of the C-terminal domain called the unadecapeptide sequence, also referred to as the tryptophan-rich loop (ECTGLAWEWWR) [81]. Since this difference abolishes the cholesterol requirement for ILY membrane binding, the unadecapeptide sequence was proposed to be a cholesterol binding site for PFO and other CDCs [80]. This hypothesis was confounded by the fact that ILY still requires membrane cholesterol for beta-barrel

formation and TM insertion [73]. More recently, a study by Soltani et al. has discovered that 3 separate short loops (L1-L3) adjacent to the unadecapeptide sequence are required to make contact with membrane cholesterol in ILY and PFO in order for TM insertion [82]. Currently, it is believed that both the unadecapeptide sequence and L1-L3 (for PFO-like CDCs) are associated with cholesterol in the membrane and this interaction is critical for formation of the TM-beta barrel and initial membrane binding.

The ability of CDCs to specifically recognize cholesterol rich regions of cells has led to the hypothesis that CDCs are targeted to and bind lipid rafts. In one study of listeriolysin O (LLO), a CDC secreted by *L. monocytogenes*, LLO was shown to cluster lipid raft markers (such as GM1, the GPI-anchored proteins, and the tyrosine kinase Lyn) in cells as the toxin oligomerized on the cell membrane [83]. Furthermore, the membrane binding domain (domain 4) of PFO has also been used as a raft probe in cellular studies as it has been shown to co-localize with raft markers (flotillin and Src family kinases) using microscopy and detergent resistant membrane studies [84-86].

Goal of this work: measuring lipid raft affinity of PFO in model membranes

As the above studies show, CDCs have been shown to localize to cholesterol rich regions of cells as measured by confocal microscopy and DRM analysis. Since CDCs are TM proteins, and exactly how TM proteins associate with lipid rafts is yet to be understood, they make an ideal family of proteins to study lipid raft affinity in model membranes. In this thesis, I have characterized the membrane and sterol binding ability of the CDC PFO in both its TM and non-TM state using fluorescence spectroscopy and model membranes. I have also measured the raft association of PFO for ordered domains using FRET as a measure of local lipid environment, and compared it to its localization to DRMs.

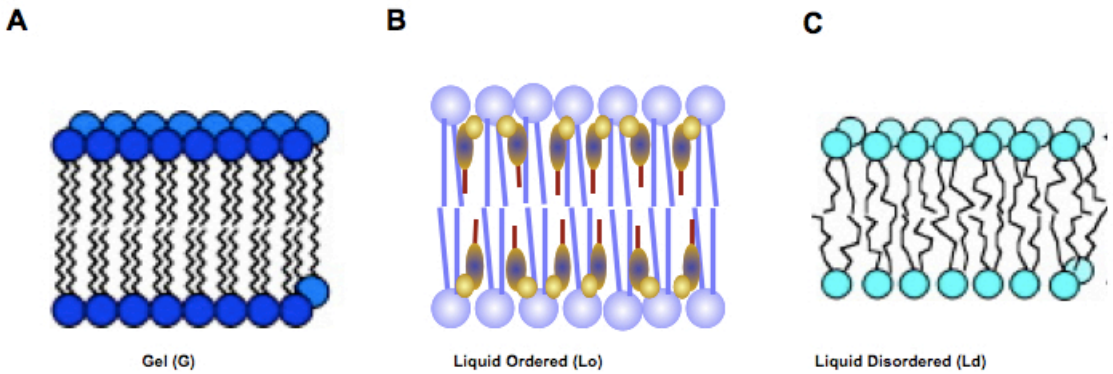

Figure 1.1: Schematic depiction of the three phases of membrane bilayers. (A) Gel phase (G) is a tightly packed state in which lateral diffusion is slow (B) Liquid ordered phase (Lo) is a tightly packed state in which lateral diffusion is fast, and (C) Liquid disordered phase (Ld) is a loosely packed state in which lateral diffusion is fast. Figure taken and adapted from *http://membranes.nbi.dk*

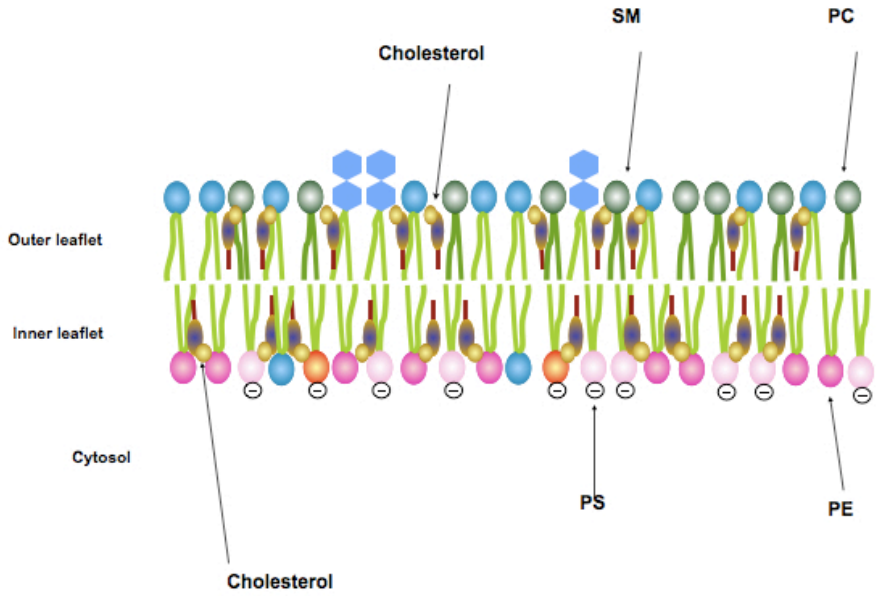

Figure 1.2: Schematic representation of asymmetry within mammalian plasma membranes. The outer leaflet is rich in sphingomyelin (SM) and cholesterol, while the inner leaflet is composed of unsaturated phosphatidylserines (PS) and phosphatidylethanolamines (PE). Drawing kindly provided by Mi Jin Son.

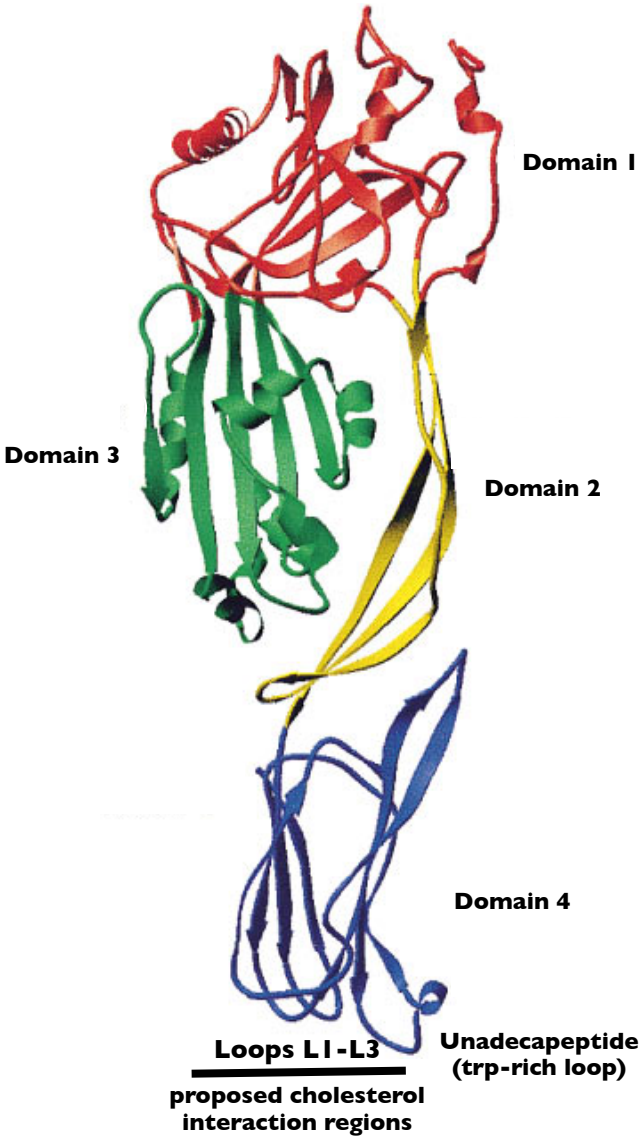

Figure 1.3: Structure of Perfringolysin O Monomer. The TRP rich motif and Domain 4 (blue) are involved in initial membrane binding. The alpha-helices within Domain 3 (green) convert into beta-strands for membrane insertion. Domain 2 (yellow) undergoes a vertical collapse to bring Domain 3 closer to the membrane surface. Figure was taken from Rossjohn, et al. and adapted. [75]

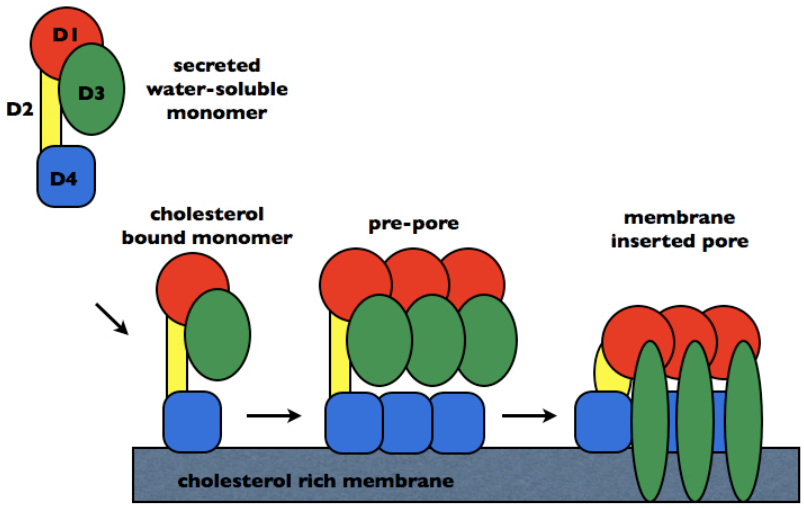

Figure 1.4: Model for CDC pore formation. A CDC is secreted as a water soluble monomer. It binds to cholesterol on the surface of the membrane, presumably as a monomer. It oligomerizes on the membrane surface forming a pre-pore structure, and then inserts into the membrane forming a pore. This figure was adapted from Giddings, et al [74].

CHAPTER 2
Materials and Methods

Materials: Unlabeled phospholipids, cholesterol,1,2-di(9,10)bromostearoyl-*sn*-glycero-3-phosphatidylcholine (BrPC), ganglioside GM1, and 1,2-dioleoyl-N-pyrenesulfonyl phosphatidylethanolamine (pyrene-DOPE) were purchased from Avanti Polar Lipids (Alabaster, AL). 1,2-dipalmitoyl-N-pyrenesulfonyl phosphatidylethanolamine (pyrene-DPPE) was purchased from the Molecular Probes Division of Introgen (Carlsbad, CA). Radiolabeled lipids were purchased from American Radiolabeled Chemicals (St. Louis, MO). 22-(Diphenylhexatrienyl)-docosyltrimethyl ammonium, (LcTMADPH) was a gift of G. Duportail and D. Heissler (Université Louis Pasteur, Strasbourg). Lanosterol ("97 % pure") and β-sitosterol were purchased from Sigma-Aldrich (St. Louis, MO). All other sterols were purchased from Steraloids (Newport, RI). . Lipids were stored dissolved in ethanol or chloroform at -20°C. Concentrations were determined by dry weight (for pyrene-DPPE and pyrene-DOPE by absorbance using an ε of 35,000 $cm^{-1}M^{-1}$ at 350 nm, for LcTMADPH by absorbance using an ε of 100,000 $cm^{-1}M^{-1}$ at 358 nm). BODIPY-FL labeling reagent and Streptavidin BODIPY-FL conjugate (BOD-SA) (discontinued except as a custom labeling product) were purchased from Invitrogen (Carlsbad, CA), and the latter reconstituted with water to give a 100 μM solution. Biocytin (ε-biotinoyl-L-lysine) was purchased from Anaspec (San Jose, CA). Acetyl-$K_2W_2L_8AL_8W_2K_2$-amide (LW peptide) was purchased from Invitrogen (Carlsbad, CA) and used without further purification. Triton X-100 (scintillation grade) was purchased from Yorktown Research (Hackensack, NJ). cholera toxin B was purchased from EMD Chemicals (Gibbstown, NJ). TALON bead resin was purchased from Clontech (Mountain View, CA). All other chemicals were reagent grade.

Sterol purity was analyzed on HP-TLC plates (Merck & Co, Whitehouse Station, NJ). Approximately 2 μg of sterol dissolved in ethanol was applied to the plate, dried, and then chromatographed using a sequential solvent system. The first solvent (50:38:3:2

(v:v) chloroform/methanol/acetic acid/water) was allowed to migrate halfway up the plate. The plate was then dried, introduced into a second chamber containing the solvent system 1:1 hexane/ethyl acetate (v:v), and chromatographed until the solvent migrated to near the top of the plate. For each step, solvent chambers were equilibrated with solvents for at least 2 h before chromatography. The plate was then dried and sprayed with 5% (w/v) cupric acetate, 8% (v/v) phosphoric acid in water. To detect sterol, plates were charred at 180 °C for 5 min. Sterols deemed impure (zymosterol and desmosterol) were purified by TLC [35], and purity was confirmed by HP-TLC.

A functional cysteine-less derivative of wild type PFO (PFO C459A), a pre-pore mutant (PFO C459A Y181A) (MUT PFO), and a cysteine mutant (PFO C459A E167C), (the latter two gifts of A. Heuck, U. Mass. Amherst) were expressed in *E. coli* as described previously [87]. Both WT and pre-pore PFO were then purified by a modification of the previously reported protocol [87]**.** Three hours after induction of expression with 1mM IPTG, two liters of cultured *E. coli* expressing PFO were pelleted at 4°C. Protein production was induced by adding IPTG to a final concentration of 1 mM**.** The bacteria were resuspended in NiA buffer (10 mM MES, 150 mM NaCl, pH 6.5) containing 150 µg/ml PMSF and 100 µg/ml chicken egg white lysozyme (Sigma-Aldrich), incubated for 30 min at room temperature, subjected to tip sonication with a cell disruptor (Heat Systems, Ultasonics, Inc, Plainview, NY) for 15 s while cooled on ice, and then cooled a further 15 s. The sonication and cooling steps were repeated two times. Next, the mixture was spun down at 15,000 rpm in a SS-34 rotor at 4°C using a Dupont RC-5 centrifuge. The supernatant from this step was incubated for 20 min. at room temperature with TALON metal affinity resin (3 mls). Resin was then pelleted with a tabletop centrifuge, added to a 0.8 X 4 cm poly-prep plastic column (Bio-Rad, Hercules, CA), washed with about 5 ml NiA buffer, followed by a 1 ml aliquot of NiA buffer

containing 50 mM, and then a 1ml aliquot of NiA buffer containing 100 mM imidazole. The PFO was then eluted with several 1 ml aliquots containing NiA buffer with 400 mM imidazole. Fractions containing PFO were pooled and dialyzed overnight in 4 L of Buffer B (10 mM MES, 1 mM EDTA, pH 6.5, + 0.5 mM DTT for cys-containing PFO) with one buffer change. The pooled PFO-containing fractions were then subjected to gravity anion-exchange chromatography using SP-Sephadex resin (GE Healthcare, Piscataway, NJ) in a 0.8 x 4 cm poly-prep plastic column and stepwise eluted 1ml aliquots of Buffer B containing increasing concentrations of NaCl in 100 mM steps, with duplicate aliquots at 200mM and 300mM NaCl. The majority of purified PFO eluted in Buffer B containing 300-400 mM NaCl. It was then dialyzed against PBS pH 7.4 (10 mM sodium phosphate, 1 mM potassium phosphate, 137 mM sodium chloride, 13 mM potassium chloride), and stored at -20°C.

Labeling of PFO (C459A E167C)with BODIPY

1 mg/ml of purified PFO (C459A, E167C) was incubated at 4°C (with 22 µl of 10 mM solution of BODIPY-FL (in DMSO) for 2 hours on shaker. The reaction mixture was then chromatographed on a Sephadex-G50 1 x 20 cm column with a 13 ml bed volume and eluted in 1 ml fractions. Labeled protein eluted in fractions 5-12, with the majority of labeled protein in fraction 6, as measured by absorbance of Trp and BODIPY. Fraction 6 was then dialyzed overnight at 4°C against 6L of 1X PBS with 1 buffer change to remove any excess BODIPY. Both labeled and unlabeled PFO (C459A E167C) were found to bind to cholesterol containing vesicles to the same extent as unlabeled PFO (C459A) and PFO (C459A Y181A) as measured by the binding assays described below.

Preparation of Liposomes

Multilamellar vesicles (MLV) were prepared at a concentration of 500 μM lipid (or 25 mM lipid for raft affinity FRET and DRM binding assays) in PBS pH 7.4 or 5.1 (PBS at pH<7.4 being prepared by titrating PBS pH 7.4 with acetic acid) similarly as described previously [40]. Dried lipid mixtures (redissolved in $CHCl_3$ and redried under N_2 and then high vacuum for at least 1 h) were dispersed in buffer at 70 °C and agitated at 70°C for 15 min using a VWR multitube vortexer (Westchester, PA) placed within a convection oven (GCA Corp, Precision Scientific, Chicago, IL). The samples were then cooled to room temperature. Large unilamellar vesicles (LUV) were prepared from MLV (prepared at a lipid concentration of 10 mM) by subjecting the MLV to 7 cycles of freezing in a mixture of dry ice and acetone for 30 s and thawing at room temperature. Small unilamellar vesicles (SUV) were prepared at a concentration of 100 μM lipid in PBS (pH 7.4, 6.8, or 5.1) by ethanol dilution in a manner similar to that described previously [40]. [SUV samples for quenching experiments in Chapter 3 contained 5 μM pyrene-DPPE in addition to 100 μM unlabeled lipids.] Lipids mixed in ethanol were diluted slightly more than 50-fold in PBS buffer heated to 70 °C, briefly vortexed, incubated at 70°C for about 5 min, re-vortexed, and then cooled to room temperature.

Fluorescence Intensity Measurements

Fluorescence emission intensity was measured at room temperature on a SPEX Fluorolog 3 spectrofluorimeter. For fixed wavelength measurements, excitation and emission wavelength sets used (in nm) were (295,340) for tryptophan, (485,518) in Chapter 3 and (488,515) in Chapter 4 for BODIPY-FL labeled streptavidin and BODIPY-FL labeled PFO, (334, 384) for pyrene-DOPE, and (358, 427) for LcTMADPH. Samples for raft affinity FRET experiments were prepared in triplicate, duplicate samples were prepared for fluorescence measurements in all other experiments. Fluorescence intensity

in single background samples lacking fluorophore was subtracted. For protein emission spectra, samples and backgrounds were excited at 280 nm and emission was acquired from 300-400 nm.

Vesicle Binding Experiments

The ability of PFO to associate with vesicles was assessed by measuring the increase in intrinsic Trp emission intensity which occurs when the Trp residues located within domain 4 come into contact with sterol-containing membranes [88]. Unless otherwise noted, PFO (5 µg from a stock solution containing ~1-2 mg/ml protein) was added to 1 ml unilamellar vesicle preparations at the desired pH (5.1, 6.8 or 7.4) and lipid composition, allowed to incubate for 1.5-2 h at room temperature, and then fluorescence emission intensity was measured as described above.

Binding and Oligomerization Assays

To assess PFO oligomerization, MLV (500 µM lipid) composed of DOPC, BrPC and sterol (with BrPC being 10 mol% of total lipid) were prepared in 200 µl PBS at pH 7.4 or 5.1 (depending on desired experimental conditions) and incubated with 10 µg PFO for 1 h at room temperature. Samples were centrifuged at 14,000 rpm in an Eppendorf centrifuge model 5415C (Westbury, NY) for 20 min at room temperature. Pellets containing the MLV and bound PFO were resuspended in 20 µl PBS (pH 7.4), solubilized with 5 µl SDS loading buffer [40 % glycerol (v/v), 25% SDS (w/v), and 0.1% bromphenol blue (w/v)], and then analyzed using denaturing SDS-agarose gel electrophoresis (SDS-AGE) as described previously [87]. Briefly, 2 % (w/v) agarose gels were run for 1-1.25 hours at 103 volts in SDS gel reservoir buffer (192 mM glycine, 25 mM tris-base in 0.1% (w/v) SDS) and fixed overnight in 30% (v/v) methanol:10% (v/v) acetic acid. The gels were then dried for 3 h at 70°C in a Savant slab gel dryer

(Holbrook, NY), stained with 0.2 % (w/v) Coomassie Blue dissolved in 30% (v/v) methanol:10% (v/v) acetic acid for 2 h, and then destained for 30 min-1h in the fixing solution.

Assay for Pore Formation

PFO-induced pore formation was measured by assaying the efflux of vesicle-entrapped biocytin via the increase in the BODIPY fluorescence emission intensity upon binding of biocytin to BODIPY-labeled streptavidin (BOD-SA) in the external solution. LUVs with trapped biocytin were prepared in the presence of 537 μM biocytin by freezing and thawing MLVs (10 mM lipid), as described above. The LUVs were dialyzed against 4 L of PBS overnight with one change of dialysis buffer to remove external biocytin. 10 μl of LUVs with entrapped biocytin were diluted to a lipid concentration of 100 μM and a volume of 990 μL with PBS and then BOD-SA (10 μl from the stock solution) was added externally to the vesicles to give a BOD-SA concentration of 10 nM. BODIPY emission intensity was then measured. PFO was added to a concentration of 5 μg/ml, samples were briefly mixed, and then BODIPY intensity was monitored as a function of time for up to 45 min.

Raft affinity FRET assay

To assess PFO raft affinity, 20 μl of a 25 mM MLVs of various lipid compositions (prepared in PBS, pH 5.1) were incubated with 3 μg PFO. "F samples" had an additional amount of FRET acceptor (either 2 mol% pyrene-DOPE or 1 mol% LcTMADPH). "Fo samples" lacked energy transfer acceptor. After a 1 hr incubation at room temperature, samples were then diluted with 980 μl 1X PBS, pH 5.1. To measure cholera toxin B raft affinity, the same procedure was followed as for PFO, but vesicles contained an additional 2 mol% ganglioside GM1, 5 μg CT-B chain was added, and the

samples allowed to incubate at room temperature for 1 hour before dilution with 980 µl PBS (pH 5.1). For LW samples, LW peptide was added from a ethanol stock to lipids prior to vesicle preparation to give a final concentration of 0.25 mol% peptide. Lipid concentration was the same as in in PFO-containing samples. 20 µl of LW peptide containing vesicles were diluted with 980 µl PBS pH 5.1. Tryptophan fluorescence emission intensity was then measured for each sample and background as described above.

DRM analysis by sucrose density fractionation

To assess PFO DRM association, 20 µl of 25 mM MLVs (when desired, with trace amounts of radiolabeled ^{3}H-cholesterol, ^{14}C-dioleoylphosphatidylcholine, ^{14}C sphingomyelin, or ^{3}H ceramide) were incubated with 3 µg WT or MUT PFO mixtures (each mixture had 6:1 ratio of labeled WT PFO:unlabeled WT PFO or unlabled MUT PFO) for 1 hr at room temperature at pH 5.1, then diluted to 450 µl with pH 5.1 PBS. 100 µl of 10% (v:v) TX-100 was then added to vesicles, samples were vortexed and then allowed to incubate at room temperature for 2 h. After incubation, samples were vortexed, and then 450 µl of 80% (w:v) sucrose solution was added, and the samples were then vortexed until a uniform solution was observed. This 1 ml sample was then layered on to the bottom of a Beckman 4 ml plastic ultraclear centrifuge tube, overlayed with 1 ml 20% (w:v) sucrose, 1 ml 10% (w:v) sucrose, and finally 1 ml 5% (w:v) sucrose (with all overlaying sucrose solutions also containing (0.2% (v:v) TX-100). These samples were then spun for 2 h in a Beckman L8-85 ultracentrifuge at 42,000 rpm at 4°C . After spinning, gradients were fractioned into six 667 ul fractions from the top of the gradient to the bottom. 10 µl from fractions 2 and fractions 5 were removed for refractive index was measurements, and then samples were diluted to 1 ml with PBS pH 7.4, after which fluorescence intensity (of BODIPY-labeled PFO, LcTMADPH, and/or

pyrene-DOPE) measured. If radiolabeled lipids were present, 3 ml of scintillation fluid (Sigma Ultima Gold cocktail) was added to each entire fraction and radioactivity measured in a Beckman Coulter LS 6500 scintillation counter.

CHAPTER 3

Effect of sterol and phospholipid structure on PFO membrane interaction

INTRODUCTION

The cholesterol dependent cytolysins (CDCs) are a family of bacterially secreted pore-forming proteins that require cholesterol in order to function [89]. Perfringolysin O (PFO) is a CDC which contributes to the pathogenesis of the anaerobic gram-positive bacterium *Clostridium perfringens* [90]. While PFO has been presumed to act extracellularly on immune cells [90], it has more recently been shown to be necessary for both phagocytic escape and survival of C. *perfingens* within host macrophages [91].

PFO contains four domains. Secreted as aqueous monomers, PFO recognizes membrane cholesterol through a tryptophan-rich motif within Domain 4 [84, 92]. Once associated with the membrane, PFO oligomerizes into complexes of 20-50 subunits (forming a "pre-pore" structure) [73]. In the pre-pore state, the insertion domain (Domain 3) is held ~60 Å above the surface of the membrane by Domain 2 [93]. To induce pore formation, Domain 2 undergoes a "vertical" collapse upon pore formation which brings Domain 3 within range to insert into the bilayer [78]. Additionally, a major structural rearrangement takes place within Domain 3 whereby six α-helices rearrange into two amphipathic β-hairpins that insert into the membrane to form a transmembrane (TM) structure [78]. The resulting pore ranges in size from 250-300 Å in diameter [73].

While cholesterol has been presumed to be the cellular receptor for PFO and some other CDCs [92], how PFO binds cholesterol has yet to be fully explained. Studies using model membrane systems typically require considerably high concentrations of cholesterol (up to 50 mol%) in order for efficient pore formation by CDCs [94]**.** Recent studies also show that only the tip of Domain 4 is exposed to the nonpolar core of the bilayer [79, 95]. A model in which PFO binds to a membrane surface involving several

sterol molecules has recently been proposed [96]. Additionally, cholesterol is required for the PFO pre-pore to pore conversion, and has also been shown to be necessary for pore formation by intermedilysin, a related CDC which does not use cholesterol as a receptor, but requires it for pore formation [73].

CDC proteins are also of interest because they are believed to bind to lipid rafts via their affinity for sterol. Lipid rafts are tightly packed sphingolipid and sterol-rich liquid-ordered (Lo) membrane domains which are believed to co-exist in eukaryotic cellular membranes with loosely packed disordered (Ld) domains composed mostly of unsaturated lipids (for recent reviews see [25, 97]). Rafts are believed to serve many functions in cellular processes at the plasma membrane and have been proposed to serve as platforms that regulate protein-protein interactions [1]. While these lipid domains have been highly studied in model membranes, where their existence is widely accepted, their formation and functional role in cells remains controversial**.** Both intact PFO and isolated Domain 4 have been used as markers of cholesterol-rich regions of cell membranes [84-86].

The details of PFO-raft affinity are of particular interest because PFO is a TM protein, and the origin of TM protein-raft affinity is not clear. Although biochemical studies detect TM proteins within detergent-resistant membranes that may be derived from ordered domains in cells, TM proteins should not be able to pack well with lipids in an ordered state [65], and the origin of their association with rafts is unclear. Since the TM insertion of PFO can be controlled, it is an ideal protein to study this question. Furthermore, like other CDC's, PFO interaction with membranes is affected by sterol structure [77, 98-102], and the relationship between the raft-forming abilities of sterols

[35-38] and sterol interaction with PFO should yield useful information on PFO affinity for rafts.

In this study we found that the interaction of PFO with membranes does not require that the sterol to which it binds has the ability to promote raft formation. Furthermore, tightly packing phospholipids, which interact strongly with sterols, tended to weaken the PFO-membrane interaction. These results do not mean that PFO does not interact with rafts, but, together with the observation that a pre-pore mutant has a similar sterol specificity as "wild-type" protein, it does place important constraints on the origin of PFO affinity for rafts. In the course of these experiments we also found that a low pH strongly promoted the interaction of PFO with membranes. Combined with recent cellular studies [91], this supports the hypothesis that at least one physiological function of PFO involves low pH.

RESULTS

PFO interacts with membranes at both low and neutral pH.

Since low pH-induced unfolding often aids protein toxin insertion into membranes, we compared the behavior of PFO at low and neutral pH. First, the interaction between (Cys-less) PFO and model membrane vesicles was measured. [The removal of the Cys eliminates the sensitivity of PFO to spontaneous inactivation by oxidation [103].] Previous studies have shown that the interaction of PFO with membranes can be detected by the large increase in Domain 4 Trp emission intensity that accompanies association with membranes [88]. A similar (four-fold) increase of Trp emission intensity relative to that in aqueous solution is observed when PFO is incubated with vesicles at pH 7.4 and pH 5.1, suggesting PFO interacts with membranes in a similar fashion at low and neutral pH (Figure 3.1). Notice that there is a small red shift in the emission spectrum at low pH in aqueous solution relative to that at neutral pH. This is consistent with an increased Trp exposure to a polar environment, e.g. aqueous solution, at low pH, and suggests that there is a small unfolding event at low pH. In the presence of lipid vesicles, this red shift is not observed, and spectra at low and neutral pH are nearly identical.

The kinetics of PFO interaction with vesicles at neutral and low pH were also compared. Measurements of the time dependence of the increase in emission intensity upon incubation of PFO with vesicles demonstrates that PFO-membrane binding occurs faster at pH 5.1 ($t_{1/2}$= 1.5 min) than at pH 7.4 ($t_{1/2}$ = 6.5 min) (data not shown). A similar difference in the rate of interaction at pH 5.1 and 7.4, is observed at 37^{o}C, although the half-times for membrane interaction decrease by a factor of about two relative to those at room temperature and the increase in fluorescence is about three-fold (data not shown).

PFO-vesicle interactions at low pH occur at lower cholesterol concentrations than at neutral pH.

The above results suggest that low pH might enhance the interaction PFO with membranes. To examine this, the interaction of PFO with vesicles containing various amounts of cholesterol was compared at low and neutral pH. Figure 3.2A shows that the cholesterol concentration that induces PFO interaction with DOPC:cholesterol vesicles is less at low pH than at neutral pH, with the increase in fluorescence emission intensity being half-maximal at 15-20 mol% cholesterol at pH 5.1 (o) and 25-30 mol % cholesterol at pH 7.4 (•).

It is possible that binding to vesicles might occur without an increase in Trp fluorescence emission intensity. To confirm that the increase in Trp fluorescence emission intensity accurately reports when binding to vesicles occurs, more direct methods were used. First, a pyrene-labeled lipid was used as a fluorescence resonance energy transfer (FRET) acceptor for Trp, and binding as a function of cholesterol concentration assayed via the amount of FRET, as detected by quenching of Trp fluorescence emission intensity. Figure 3.2B shows that the cholesterol concentration dependence of Trp fluorescence quenching is very similar to the cholesterol dependence of the Trp intensity increase in the absence of acceptor, with lipid interaction occurring at a lower cholesterol concentration at low pH than at neutral pH. As commonly observed [104], FRET-induced quenching is incomplete because not all of the donors are close enough to the pyrene-labeled lipid to take part in energy transfer. Thus, the maximal level of FRET-induced quenching, 80%, presumably represents complete binding of PFO to the vesicles. It should also be noted that the small amount of apparent FRET at low cholesterol concentration is largely an inner filter artifact arising from a small amount of pyrene absorbance.

These results were further confirmed by measuring the association of PFO with vesicles via centrifugation of PFO mixed with MLV. The amount of bound PFO in the MLV-containing pellet was detected by agarose gel electrophoresis in SDS (SDS-AGE). The cholesterol concentration dependence of PFO binding detected by sedimentation (Figure 3.2C) is similar to that obtained from fluorescence intensity measurements in terms of the threshold sterol concentration for binding PFO and its pH-dependence. The position of the main PFO band on the gels indicates that when membrane-bound, PFO efficiently forms characteristic SDS-resistant oligomers [87] at both pH values (although a variable amount of monomers can be occasionally observed).

PFO forms pores efficiently at low pH.

While the experiments above show that PFO exhibits similar binding and oligomerization behavior at low and neutral pH, under some circumstances PFO can form pre-pore oligomers that do not deeply membrane-insert [87]. We therefore investigated whether PFO pore-forming behavior is retained at low pH. To assay pore formation, we measured the efflux of biocytin encapsulated inside LUVs. In this method, efflux is detected by the increase in the BODIPY emission intensity that occurs when biocytin binds to BODIPY-tagged streptavidin added externally to the vesicles [105-107]**.**

Figure 3.3 shows that PFO forms pores efficiently in DOPC vesicles containing 50 mol% cholesterol at both pH 5.1 and 7.4, with the rate of biocytin efflux being slightly faster at low pH. The difference between neutral and low pH is even larger at lower cholesterol concentrations, presumably because PFO binds to a greater extent at low pH than at neutral pH (data not shown). Figure 3.3 also shows no pore formation occurred in the absence of cholesterol.

A control experiment using a previously identified mutant (PFO C459A,Y181A) that remains in the pre-pore state [108], shows a lack of pore formation at both low and neutral pH (Figure 3.3A and B). This confirms the validity of the pore-formation assay, and shows that the difference in pre-pore mutant and wild-type PFO behavior is retained at low pH.

We conclude that the structure and membrane interactions of PFO at low and neutral pH must be very similar, although low pH enhances PFO membrane interaction and function.

Effect of sterol structure upon PFO-membrane interaction: Fluorescence studies.

It has been proposed that PFO binds to cholesterol-enriched ordered domains (lipid rafts) [85]. Prior studies of sterol specificity have shown that sterol structure is important for interaction with PFO, but have not established whether or not PFO interacts most strongly with sterols promoting lipid raft formation [99]. To investigate this, the interactions of PFO with sterols and sterol derivatives that either strongly stabilize ordered domain formation (cholesterol, dihydrocholesterol, epicholesterol, lathosterol, sitosterol [35-38]), weakly stabilize or have little effect of the stability of ordered domain formation (zymostenol, lanosterol, cholesteryl acetate, cholesterol methyl ether, allocholesterol [35-38]) or destabilize ordered domain formation (coprostanol [38]) were compared.

The binding of PFO to vesicles as a function of the concentration of sterol or sterol derivative in the vesicles was detected by sterol-induced increases in Trp fluorescence (Figure 3.4). At low pH (Figure 3.4A), PFO interacts well or moderately

well with sterols that strongly promote lipid-ordered domain formation (cholesterol, dihydrocholesterol, sitosterol, lathosterol), weakly stabilize ordered domain formation (desmosterol, zymostenol, allocholesterol), or do not promote raft formation (coprostanol). The interaction with coprostanol and zymostenol requires somewhat higher sterol concentrations than is required for the other sterols. PFO does not interact or interacts very poorly with epicholesterol, which stabilizes ordered domains to a significant degree [38]**,** or with lanosterol and sterol derivatives with a blocked 3-ß OH (cholesteryl methyl ether, cholesteryl acetate) that have little effect on ordered domain stability. This shows that PFO binding is not tightly correlated with the relative ability of sterols or sterol derivatives to form ordered domains.

The relative sterol specificity of PFO is similar at neutral and low pH. However, the dependence upon sterol concentration is shifted, such that much higher sterol concentrations are required to induce an increase in Trp emission intensity at neutral pH than at low pH (Figure 3.4B).

Effect of sterol structure upon PFO-membrane interactions: Centrifugation experiments.

It is possible that the apparent dependence of PFO binding to membranes upon sterol structure is not due to a lack of PFO interaction with membranes, but rather to an inability of a particular sterol to induce a conformational change that alters Trp fluorescence emission intensity. To examine this possibility, the binding of PFO to membranes and the oligomeric state of the membrane-bound PFO was determined using centrifugation and SDS-AGE. Figure 3.5 shows that at low pH there is near maximal PFO binding to vesicles containing cholesterol, dihydrocholesterol, sitosterol, or lathosterol at 20 mol% sterol, and some binding to vesicles with allocholesterol at 20 mol %. However, binding to vesicles containing coprostanol or zymostenol requires 30 mol%

sterol, and no binding to vesicles occurs even with 40 mol% lanosterol, cholesteryl acetate or cholesterol methyl ether. This order of sterol recognition by PFO mirrors that derived from Trp fluorescence emission intensity (Figure 3.4).

In every case, the bound PFO is predominantly oligomeric (Figure 3.5). It therefore appears that sterol structure does not greatly affect the ability of membrane-associated PFO to oligomerize. However, it should be noted that in several cases, there is some smearing of the oligomers on the gel at the highest sterol concentrations. The origin of this behavior is not understood.

We have also tested two additional sterols, ergosterol and 7-dehydrocholesterol, and found that they promote PFO binding to liposomes. However, this interaction was difficult to quantify because we found these sterols quench Trp fluorescence emission intensity [35], thereby masking the emission intensity increase usually observed when PFO binds to membranes. SDS-AGE showed that PFO binding and oligomer formation with liposomes containing 20 mol% of these sterols was as complete as for liposomes containing 20 mol% cholesterol (data not shown).

The sterol specificity of pre-pore PFO Y181A mutant, which cannot form a TM ß-barrel [108] was also examined. It shows a sterol specificity profile at low pH (Figure 3.6) that is almost identical to that of the Cys-less “wild type” PFO (Figure 3.4A) as judged by the dependence of Trp emission intensity upon sterol or sterol derivative concentration within vesicles. Therefore, the step that is sensitive to sterol sensitive appears to be the initial recognition and binding of the membrane surface by PFO. Once bound, PFO can spontaneously oligomerize to form pre-pore complexes.

Effect of sterol structure upon pore formation by PFO.

To determine if pore formation by PFO is also sensitive to sterol identity, DOPC vesicles encapsulating biocytin and prepared with different sterols, were exposed to PFO. Pore formation is observed at low pH with cholesterol, dihydrocholesterol (which is strongly raft promoting), desmosterol (which is weakly raft stabilizing) and coprostanol (which destabilizes rafts) (Figure 3.7). Therefore, the raft-stabilizing abilities of a sterol are not tightly correlated with its ability to support PFO-induced pore formation. Vesicles containing DOPC mixed with 40 mol% of allocholesterol or lathosterol also show a significant degree of pore formation, but no pore formation was seen in vesicles containing DOPC and 40 mol% lanosterol (data not shown)**.** The rate of pore formation is greater at 40 mol% (Figure 3.7A) than at 25 mol% for each sterol (Figure 3.7B). In agreement with the binding experiments, samples with 25 mol% coprostanol, which is an insufficient concentration to promote maximal PFO binding, show a significantly reduced rate and extent of pore formation as judged by the rate of biocytin release when compared to samples containing other sterols that promote near-maximal PFO-membrane interactions at 25 mol% (Figure 3.4A). Overall, the sterol dependence of pore formation by Cys-less PFO correlates with the level of its association with vesicles.

Effect of phospholipid structure on PFO-membrane interaction.

To assess whether PFO-membrane interactions would be affected by the relative ability of phospholipids to form ordered domains, four phosphatidylcholines with differing abilities to form ordered domains by themselves and with cholesterol were examined. These four, listed in decreasing order of ability to form ordered domains and pack tightly with cholesterol, were [33]: DPPC, which has two saturated palmitoyl acyl chains; POPC, which has a 1-position palmitoyl acyl chain and a 2-position unsaturated oleoyl acyl chain; DOPC, which has two oleoyl acyl chains; and DPhPC (diphytanoyl

PC), which has two multibranched acyl chains. As judged by the cholesterol-induced increase in Trp emission intensity (Figure 3.8) at low pH, the cholesterol concentration needed to induce PFO binding to vesicles increases with PC type in the order: DPhPC<DOPC<POPC<DPPC. This pattern indicates that PFO binds better to membranes that are loosely packed and have the least tendency to form ordered domains. This does *not* imply that PFO does not associate with lipid rafts, but does indicate that loose packing, which should increase cholesterol reactivity, promotes sterol binding to PFO (see Discussion).

PFO interactions with vesicles in which 50 mol % dioleoyl phosphatidylethanolamine (DOPE), or 10-30 mol % diphytanoyl PE, or 5- 20 mol % palmitoyl (C16:0) ceramide were substituted for an equal mol% of DOPC were also examined. In all of these cases, there is a decrease in the % cholesterol need to induce PFO association with membranes (data not shown). These results are also consistent with a model in which cholesterol reactivity in membranes is an important parameter controlling association with PFO (see Discussion).

Dependence of PFO interactions with vesicles on pH: Physiological implications.

To ascertain how membrane composition affects the pH dependence of PFO-membrane interactions, vesicles were prepared with various phospholipids and cholesterol concentrations. The pH dependence of Trp fluorescence was then measured to identify the pH at which membrane interaction was maximal. Figure 3.9A shows that PFO binding to vesicles containing POPC: cholesterol (7:3, mol: mol), DOPC: cholesterol (4:1), or DPhPC: cholesterol (17:3) is maximal over a broad low pH plateau. To better define the likely pH maximum under physiological conditions, the pH dependence of PFO-membrane interaction was then measured in vesicles containing a

1:1:1 molar ratio of sphingomyelin (SM): POPC: cholesterol, a mixture which mimics the outer (exofacial) leaflet of mammalian membranes. Figure 3.9B shows the binding of PFO to these vesicles has a somewhat sharper pH maximum near pH 5.5-6. Figure 3.9B also shows that in SM: POPC: cholesterol vesicles in which cholesterol concentration is decreased to 25 mol%, there is an even sharper pH maximum of membrane interaction at just below pH 6. These results are consistent with the hypothesis that PFO functions in macrophage phagosomes, as phagosomes have a luminal pH between 5 and 6 [109] (see Discussion).

Negatively charged lipid enhances binding of PFO to vesicles.

Rossjohn et al [76] very recently observed conformational changes in the PFO crystal structure at low pH, and suggested that these changes might aid PFO insertion into membranes at neutral pH when PFO encounters a membrane rich in anionic lipids, because the surface of anionic lipid vesicles have a lower "local" pH than that of the bulk aqueous solution. To determine if anionic lipid promotes PFO-membrane interactions, the binding of PFO to vesicles containing POPC and cholesterol with and without 20 mol % of the anionic lipid 1-palmitoyl-2-oleoyl phosphatidyl-L-serine (POPS) was compared (Figure 3.10). At neutral pH, PFO interacts with vesicles at a slightly lower cholesterol concentration in the presence of POPS (▲) than in its absence (Δ). However, at low pH (5.1) the presence of POPS (■) results in an even larger decrease in the mol% of cholesterol required for PFO binding to vesicles. Very similar results were obtained by incorporating 20 mol% of the anionic lipid 1,2-dioleoyl phosphophatidyl-*rac*-1-glycerol)] into vesicles with DOPC (data not shown). Thus, anionic phospholipids facilitate PFO binding, although the ability to do so at low pH suggests factors in addition to local surface pH effects may be involved.

DISCUSSION

Low pH and PFO Function: Physiological Significance and Structural Origin of Low pH Enhanced Activity.

Although one early experiment hinted that PFO retains the ability to induce hemolysis at low pH [110], it has been generally assumed that PFO acts by punching holes in the plasma membrane [90]. However, it has recently been found that PFO is necessary for escape from the phagocytic vesicles of macrophages, suggesting an internal site of action instead of, or in addition to, plasma membranes [91]. Our studies are consistent with this model. We find that PFO is significantly more active at low pH than neutral pH, suggesting that its primary site of action is in mildly acidic vacuoles. Since phagosomes are mildly acidic (pH 5.4±0.4, [109]), this is consistent with the model that phagosomes are a primary site of action. However, unlike listeriolysin O, a CDC that functions much better at low pH than at neutral pH [111], PFO is highly active at neutral pH. Thus, it seems very possible that PFO acts both in acidic vacuoles and at the plasma membrane.

How does low pH promote PFO interactions with the membrane? For acid-triggered toxins such as diphtheria toxin, low pH triggers a partial unfolding event that reorganizes the protein and thereby primes the membrane-penetrating sequences for insertion [112, 113]. This may also be the case for PFO. Recent crystallographic studies have proposed that low pH-induced conformational changes in Domains 2 and 3 prime PFO for membrane insertion by loosening a critical hinge region [76]. In addition, the low pH-triggered changes in Trp fluorescence emission intensity in the absence of lipid indicate that the PFO Trps are more exposed to the aqueous environment at low pH, a result consistent with some degree of unfolding [114]. It should be noted that the

unfolding event that occurs at low pH is likely to be local. We were unable to induce PFO insertion into model membrane vesicles using conditions that induce more global unfolding, i.e. high temperature or urea (data not shown).

Effect of Phospholipid Structure Upon PFO- Membrane Interactions: Implications for Sterol Binding.

Another striking result was that PFO interactions with sterol are inversely related to the packing properties of the phospholipids. Specifically, the looser the packing of the phospholipids [115], the lower the concentration of cholesterol needed to induce insertion of PFO into the lipid bilayer. This behavior can be explained in terms of the effect of loose packing upon cholesterol chemical reactivity. The reactivity of membrane-associated cholesterol (as judged by its activity coefficient) should be increased by exposure to aqueous solution. The "umbrella model" postulates that the headgroups of phospholipids and sphingolipids act like umbrellas, limiting the exposure of the hydrophobic portions of cholesterol to water (cholesterol having too small a polar headgroup to fully shield itself from aqueous solution) and thus reducing its reactivity [39]. Acyl chain and headgroup structures that limit the ability of cholesterol to pack closely with phospholipids should limit this shielding of cholesterol from water, thereby increasing cholesterol reactivity and thus its tendency to bind to other molecules. This effect can be very marked, and has been successfully invoked to explain how lipid structure can modulate cholesterol interaction with lipid rafts and with other toxins [40, 116].

It is also significant that we have identified conditions in which only relatively low concentrations of sterols (as low as 10-15 mol%) are required for PFO binding membranes. Studies involving PFO and model membrane systems have typically used

liposomal formulations that required very high cholesterol concentrations (about 50 mol %) to achieve efficient binding, oligomerization, and pore formation [94]. Our study shows that there is no absolute requirement for a very high concentration of cholesterol. This result has practical importance because it will allow study of PFO-membrane interactions over a much wider range of *in vitro* lipid compositions.

Lipid polar headgroup structure also affected PFO-membrane interactions. Our results showed that anionic lipids can promote PFO binding to membranes. The anionic charges near the surface may redistribute the lipid components in the bilayer to alter cholesterol exposure, alter the local pH at the membrane surface, and/or interact with PFO directly or indirectly to stabilize its binding to the membrane surface. We also found that PE and ceramide decreased the % cholesterol needed to induce PFO binding to vesicles. This agrees with previous studies of PFO [117] and that of another cytolysin [116]. This behavior can be rationalized in terms of the umbrella model. The headgroup of PE is smaller than that of PC so should be less able to shield cholesterol from water, thereby increasing cholesterol reactivity. Similarly, as pointed out by Zitzer et al [116], ceramide has such a small headgroup it can even compete with cholesterol for association with umbrella-forming lipids, as has been observed in lipid rafts [40, 116].

Effect of Sterol Structure Upon PFO-Membrane Interactions: Implications for the Nature of the Sterol-Binding Site.

Another conclusion from this study is that PFO-sterol interactions show a distinct specificity in terms of sterol structure. The structure of the polar headgroup, sterol rings and aliphatic side chains all affect how much sterol is needed to induce PFO membrane binding, oligomerization, and pore formation. The most critical feature is the OH group. In agreement with previous studies [99], our study confirms that PFO requires a free OH

group in the beta OH configuration to recognize and interact with the sterol. The sterol ring structure is also important. A 5-6 double bond (cholesterol) favors PFO binding more than a double bond in the 4-5 (allocholesterol), 7-8 (lathosterol) or 8-9 (zymostenol) positions. Ring system planarity also has a significant effect, with the relatively flat dihydrocholesterol interacting with PFO better than coprostanol, an isomer of dihydrocholesterol that is highly bent between the steroid A and B rings. The methyl groups on the sterol rings, found in lanosterol, strongly interfere with PFO interactions, although this may also be partially due to the 8-9 double bond that it has in common with zymostenol. [It should be noted that the weak interaction of PFO with lanosterol is consistent with previous studies on ostreolysin [98].] Even aliphatic side chain structure had some effect, as shown by the slightly weaker interactions of PFO with sitosterol (which has a C24 ethyl group) than with cholesterol.

It would appear from these results that PFO recognizes groups all along the sterol molecule. This would be consistent with the presence of a sterol-binding pocket almost totally surrounded by residues in Domain 4 [80]. On the other hand, only the tip of Domain 4 at one end of the elongated PFO molecule is embedded in the bilayer, and this is sufficient for cholesterol recognition and binding [93, 95]. Since different sterols will occupy different steric spaces and hence will pack differently within the bilayer, bilayer surfaces will be created that differ in the exposure of the sterols, including the portions most likely to directly interact with PFO, to the aqueous solution. A bilayer-inserted sterol that is more exposed to aqueous solution will be more exposed to PFO in solution and thus interact more readily with PFO than one that is less exposed to solution. In this fashion the steric configurations of the hydrophobic portions of the various sterols would be expected to indirectly dictate the extent to which PFO recognizes the sterol molecule, even when the sterol is not totally buried within the protein. Defining the exact

molecular origin of the sterol specificity of interactions with PFO will require further studies.

Effect of Lipid Structure Upon PFO-Membrane Interaction: Implications for PFO Interaction with Lipid Rafts.

It may seem puzzling that the sterol specificity of PFO binding to membranes does not support a model in which there is a close correlation between the raft (ordered domain) stabilizing abilities of a sterol [35-38, 118] and PFO binding. Several sterols that stabilize ordered domain formation (cholesterol, dihydrocholesterol, sitosterol, lathosterol [35-37]) interact well with PFO, but epicholesterol, which also stabilizes ordered domains [38]**,** does not, and coprostanol, which destabilizes ordered domains [38], does.

However, if sterol binding enhances PFO interaction with rafts, an obvious mechanism would be that the raft-associating surfaces of the sterol remain exposed to the lipid bilayer upon binding PFO, and thus not interact with PFO. This would be analogous to the familiar mechanism by which binding to the headgroup of ganglioside GM1 anchors cholera toxin in rafts [119]**.** A sterol bound in a deep cleft within the protein could not directly aid raft association in this way. Thus, one might not expect PFO to have any strong preference for sterols that form lipid rafts.

Furthermore, we have shown that PFO insertion is triggered more readily in a loosely packed lipid environment. This behavior also does **not** imply that PFO would have a higher affinity for disordered lipid domains than for lipid raft domains. It is possible that PFO could insert into disordered domains and then move into ordered domains subsequent to insertion. Furthermore, in membranes with co-existing disordered

and ordered domains it is likely that the cholesterol concentration would be higher in the ordered domains [120, 121], and this would tend to cancel out the preference of PFO for cholesterol in a loosely packed environment. Also, it should be kept in mind that the ordered domains in cells would be more complex than in our binary lipid mixtures, and contain some unsaturated lipids that might increase PFO affinity for ordered domains. Indeed, our preliminary studies indicate that in membranes with co-existing ordered and disordered domains, PFO does have a tendency to partition into ordered domains to a significant degree (L. Nelson, A.E. Johnson and E. London, unpublished observations).

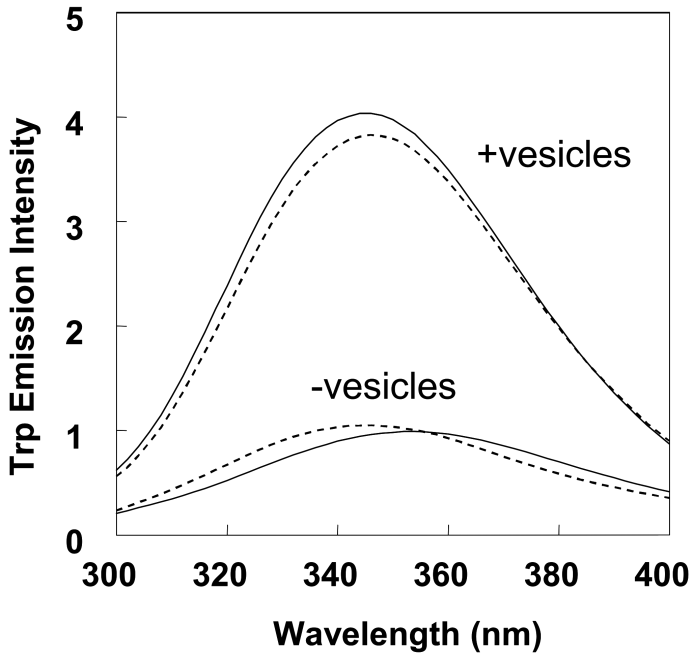

Figure 3.1: Intrinsic fluorescence emission spectra of PFO. Key: (solid) pH 5.1, (dashed) pH 7.4. At both pHs, the lower curves are in the absence of lipid and the upper curves are in the presence of 4:6 mole:mole cholesterol:DOPC vesicles. Samples in these experiments, and unless otherwise noted in all the Trp fluorescence experiments in the following figures, contained 5 μg/ml Cys-less PFO (C459A) and 100 μM lipid in the form of unilamellar vesicles prepared by ethanol dilution, and emission intensity was measured at room temperature. Spectra shown are the average from duplicate samples. Here and in the following figures, variation of Trp fluorescence intensity duplicates was very small, with values in individual samples generally within 3% of the average.

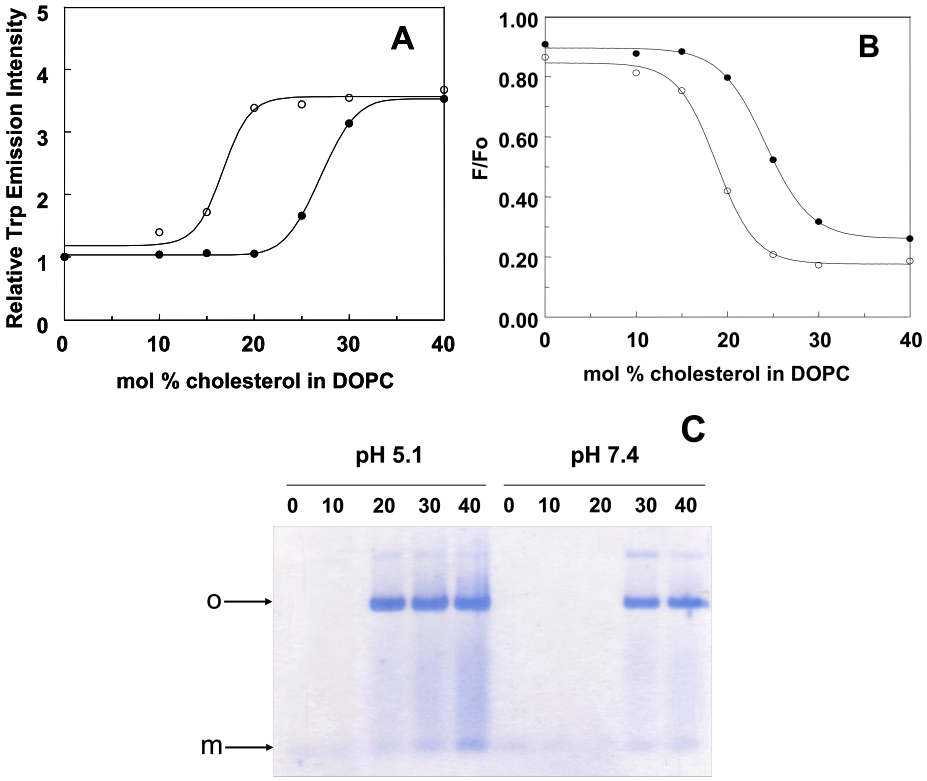

Figure 3.2: PFO interaction with model membranes occurs at lower cholesterol concentrations at low pH. (A) Effect of pH upon Trp emission intensity vs. cholesterol concentration. (●) DOPC: cholesterol vesicles at pH 7.4; (○) DOPC: cholesterol vesicles at pH 5.1. Trp emission intensity was normalized to a value of 1 in the absence of cholesterol in this and the following figures. (B) Effect of pH upon FRET-detected binding of PFO to vesicles vs. cholesterol concentration. F/Fo is the ratio of Trp fluorescence intensity in the presence of vesicles containing pyrene-DPPE (F) to that in samples without pyrene-DPPE (Fo). Samples contained a total of 100 μM unlabeled lipid (DOPC and cholesterol) with or without 5 μM pyrene-PE. The x-axis gives the mole % of cholesterol in the samples without pyrene-PE (●) DOPC:cholesterol vesicles pH 6.8; (○) DOPC:cholesterol vesicles at pH 5.1. (C) Effect of pH upon centrifution/SDS-AGE-detected binding of PFO to vesicles vs. cholesterol concentration. Samples of 50 μg/ml Cys-less PFO (C459A) were incubated with multilamellar vesicles (500 μM lipid) containing mixtures of cholesterol with DOPC and 10 mol% BrPC to aid pelleting. The pellet obtained after centrifugation was analyzed on SDS-AGE. Lanes 1-5 pellet at pH 5.1. Lanes 6-10 pellet at pH 7.4. Labels at left indicate migration position of : o, oligomers; m, monomers.

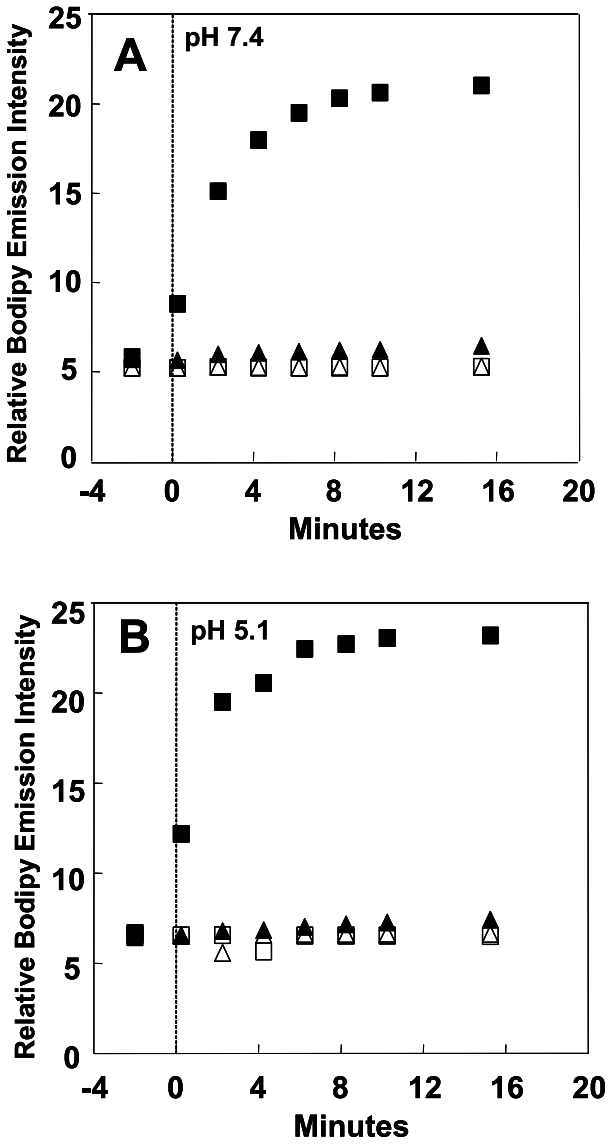

Figure 3.3: Formation of pores by PFO in large unilamellar vesicles (LUV) at neutral and low pH. (A) pH 7.4. (B) pH 5.1. Y-axis shows the increase in external BODIPY-SA emission intensity upon the release of trapped biocytin. (open symbols) DOPC; (filled symbols) 1:1 mol:mol DOPC:cholesterol; (□, ■) Cys-less PFO (C459A); (△, ▲) Cys-less pre-pore mutant (Y181A, C459A). Samples contained 100 μM lipid and 10 nM BODIPY-tagged streptavidin added externally to LUV containing entrapped biocytin. BODIPY fluorescence was measured as a function of time after the addition of 5 μg/ml of PFO. Zero time is the time of addition of PFO.

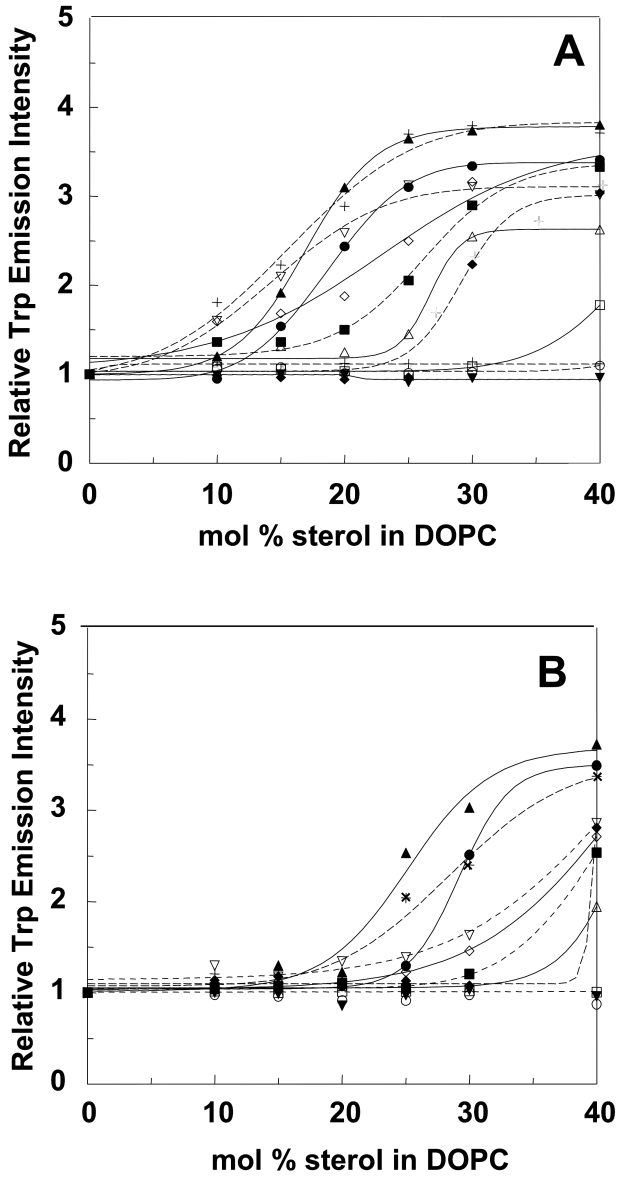

Figure 3.4: Dependence of PFO interaction with vesicles upon sterol/sterol derivative structure at neutral and low pH. (A). pH 7.4. (B). pH 5.1. Samples contained DOPC, Cys-less PFO and increasing amounts of (▲) cholesterol; (*) dihydrocholesterol; (●) sitosterol; (▽) desmosterol; (◇) lathosterol; (■) allocholesterol; (△) coprostanol; (◆) zymostenol; (□) lanosterol; (○) cholesterol methyl ether; (▼) cholesteryl acetate; or (+) epicholesterol (Figure 3.4A only). Other conditions as in Figure 3.1.

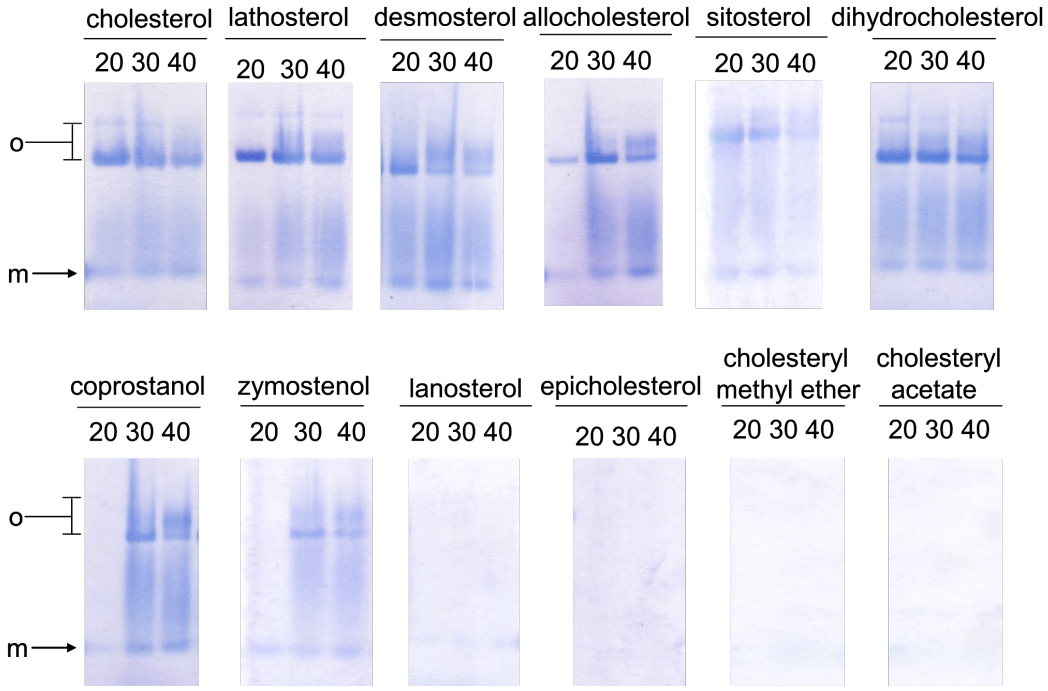

Figure 3.5: SDS-AGE analysis of PFO association with multilamellar vesicles (MLV) in the presence of different sterols/sterol derivatives at pH 5.1. The pellet obtained after centrifugation of PFO incubated with MLV (composed of DOPC:sterol or sterol derivative) was analyzed on SDS-AGE. From left to right lane for each sterol/sterol derivative concentration was 20, 30 and 40 mol%. Other experimental details as in Figure 3.2C.

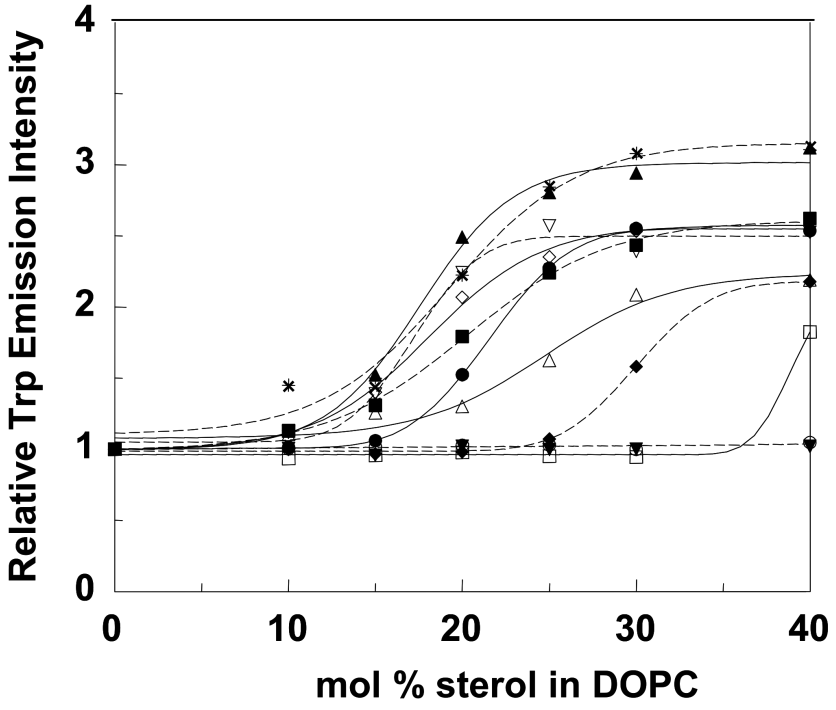

Figure 3.6: Dependence of PFO pre-pore mutant interaction with vesicles upon sterol/ sterol derivative structure at pH 5.1. Samples contained DOPC, Cys-less pre-pore (Y181A) PFO and increasing amounts of of (▲) cholesterol; (*) dihydrocholesterol; (●) sitosterol; (▽) desmosterol; (◇) lathosterol; (■) allocholesterol; (△) coprostanol; (◆) zymostenol; (□) lanosterol; (○) cholesteryl methyl ether; or (▼) cholesteryl acetate; Values for single samples are shown, except for sitosterol, zymostenol, cholesteryl methyl ether and cholesteryl acetate, which show the average value from duplicates. Other conditions as in Figure 3.1.

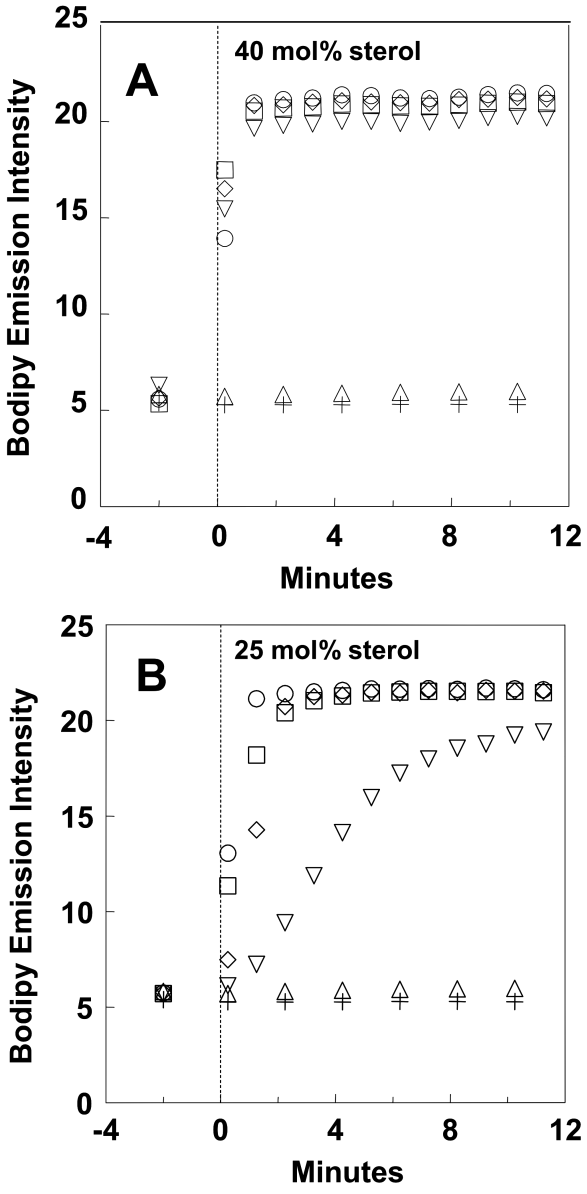

Figure 3.7: Effect of sterol structure upon formation of pores by Cys-less PFO in large unilamellar vesicles at pH 5.1. (A) Sterol-containing samples with 2:3 sterol:DOPC. (B) Sterol-containing samples with 1:3 sterol:DOPC. Y-axis shows the increase in external BODIPY-SA fluorescence upon the release of trapped biocytin. (+) no lipid; (△) no sterol; (○) cholesterol; (▽) coprostanol;(□) dihydrocholesterol; (◇) desmosterol. Other experimental conditions as in Figure 3.3.

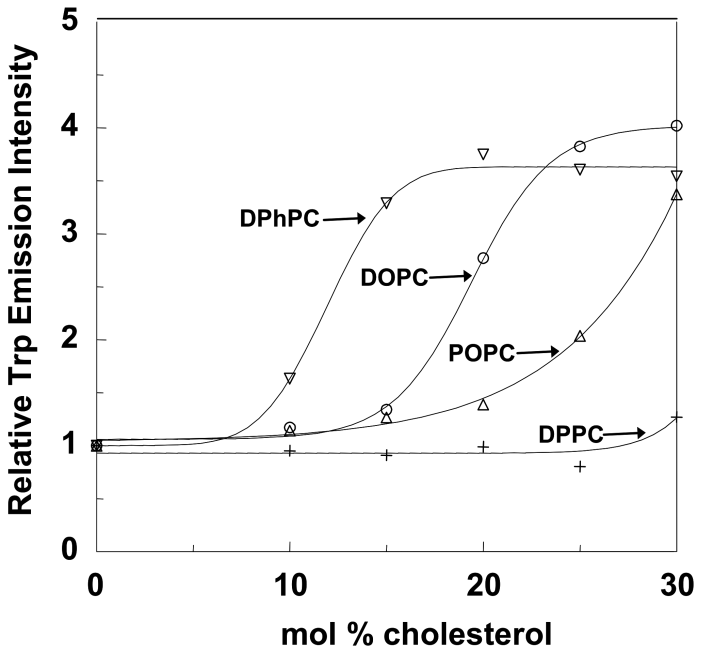

Figure 3.8: Effect of phospholipid structure upon the cholesterol concentration dependence of PFO interaction with lipid vesicles at pH 5.1. Samples contained mixtures of cholesterol with various phosphatidylcholines (PC): (▽) diphytanoyl PC; (○) DOPC, (△) 1-palmitoyl, 2-oleoyl PC (POPC), (+) dipalmitoyl PC (DPPC). Other conditions as in Figure 3.1.

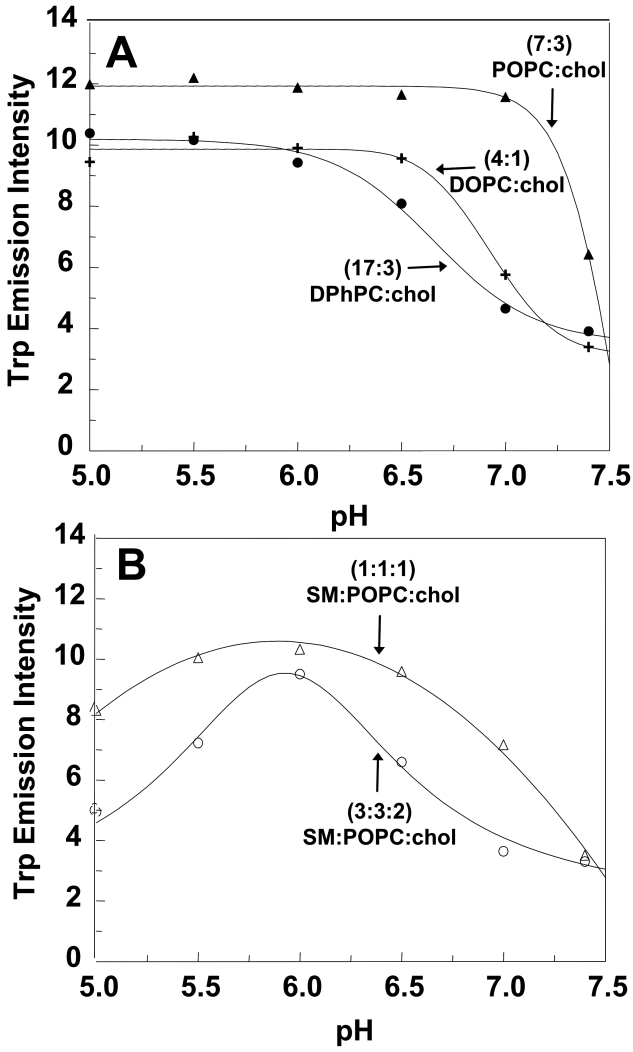

Figure 3.9: pH dependence of PFO-vesicle interactions for different lipid mixtures. (A) Binary lipid mixtures. (+) 1:4 mol:mol cholesterol:DOPC; (▲) 3:7 cholesterol:POPC; (●) 3:17 cholesterol: diphytanoyl PC. (B) Ternary lipid mixtures. (△) 1:1:1 SM:POPC:cholesterol; (○) 3:3:2 SM:POPC:cholesterol. Other conditions as in Figure 3.1.

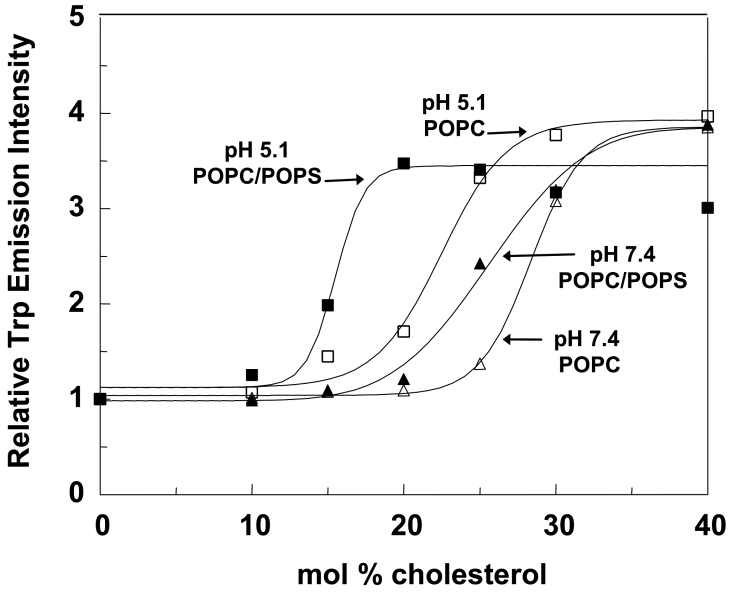

Figure 3.10: Effect of phosphatidylserine upon PFO interaction with lipid vesicles. (△)POPC:cholesterol, pH 7.4; (▲) 20 mol% 1-palmitoyl, 2-oleoyl phosphatidylserine:POPC: cholesterol, pH 7.4. (□) POPC:cholesterol, pH 5.1; (■) 20 mol% 1-palmitoyl, 2-oleoyl phosphatidylserine:POPC: cholesterol, pH 5.1. Other conditions as in Figure 3.1.

CHAPTER 4

PFO raft affinity and its dependence on lipid composition

INTRODUCTION

Perfringolysin O (PFO) is a member of a family of cholesterol-dependent cytolysins (CDCs). CDCs are beta-barrel forming toxins that require high concentrations of cholesterol in order to form large pores in cellular membranes (reviewed in [89]). PFO binds to membrane cholesterol, oligomerizes into a pre-pore structure (composed of up to 50 monomers), and this pre-pore intermediate then undergoes structural changes to form a transmembrane beta-barrel [73].

Lipid rafts are ordered membrane regions composed primarily of saturated sphingolipids and cholesterol, and are believed to co-exist with disordered domains. Since CDCs bind to cholesterol-rich membranes, it is believed they bind to lipid rafts in cells. Indeed, in a recent study, the CDC listeriolysin O was shown to co-localize with lipid raft markers (such as raft-associated tyrosine kinases) upon oligomerization in cells [83, 122]. In addition, derivatives of PFO which do not form TM pores have also been shown to co-localize with lipid raft markers, and have been found in detergent resistant membranes (DRMs) derived from cells [84-86].

Recent work in model membranes, however, has shown that PFO binds to and forms pores more readily in vesicles composed of unsaturated lipids [123, 124]. Tightly packing phospholipids, which interact strongly with sterols, have been shown to interfere with the interaction of PFO with membranes. There are no studies that have addressed PFO raft affinity directly using model membranes. This is mainly due to the requirement of extremely high cholesterol concentrations within model membrane vesicles in order to get PFO in its fully bound, oligomeric, and pore-forming state. In our previous study, we

discovered that low pH (5.1) lowers the cholesterol requirement for PFO, and this allows us to study PFO raft affinity in physiologically relevant lipid compositions [124].

In this study we measured the raft affinity of PFO in model membranes with a novel fluorescence resonance energy transfer (FRET) assay using both one energy acceptor that has a preferential affinity for Ld domains, and another energy acceptor that has a preferential affinity for Lo domains. Using this FRET assay, and comparing the behavior of the wild-type protein with a mutant that is deficient in forming the TM structure, we have observed that formation of the beta-barrel reduces raft affinity of PFO. We also observed that PFO associates with DRMs, consistent with PFO studies in cells which show a DRM association.

We also found the overall raft affinity of both the WT and the mutant PFO was reduced in some lipid mixtures where cholesterol concentrations in ordered domains was low. However, in ceramide-containing lipid mixtures, cholesterol was displaced from ordered domains, but PFO was not. Combined, these results suggest the raft affinity of PFO is not solely dependent upon cholesterol concentrations within ordered domains, but also upon the ability of the complex of PFO and bound cholesterol to pack well within ordered domains.

RESULTS

Measuring lipid raft affinity of PFO using FRET

To measure raft affinity of PFO, we developed a novel fluorescence resonance energy transfer (FRET) assay. As illustrated in Figure 4.1, the basis of our FRET analysis was to compare the amount of energy transfer in two membranes, one with Ld and Lo domains, and another homogeneous membrane that is entirely Ld. If there is partitioning of either the fluorophore (i.e. PFO or other Trp-containing proteins) and the FRET acceptor into one type of domain, there will be a difference in the local FRET acceptor concentration in relation to the fluorophore. We detect FRET from the degree of quenching of donor (Trp) fluorescence by the acceptor.

To calculate the local FRET acceptor concentration, we use an adaptation of Perrin's equation for quenching in two dimensions [125, 126] :

$$F/Fo = e^{-\pi C R_c^2}$$

where F/Fo is the ratio of fluorescence of a sample containing FRET accepter to the fluorescence of a sample lacking FRET acceptor, Rc is the radius of quenching. The expression πR_c^2 represents a circle around the quencher within which fluorescence is completely extinguished. C is the concentration of FRET acceptor.

Solving this equation for C, we get the equation:

$$C = \ln (F/Fo) / -\pi R_c^2$$

This is the concentration of the quencher surrounding the fluorophore. We can not measure Rc directly. However, if we take the ratio of C for membranes containing Lo and Ld domains (C_{Lo+Ld}) to C for homogeneous membranes (C_{Ld}), we can eliminate Rc as a parameter.

$$C_{LoLd}/C_{Ld} = \ln (F/Fo)_{LoLd} \ / \ln (F/Fo)_{Ld}.$$

Since we can measure F/Fo experimentally in each of these samples, we can calculate C_{Lo+Ld}/C_{Ld}. We call this parameter Q_L, and it represents the local FRET acceptor concentration surrounding the fluorophore in membranes containing a mixture of Lo and Ld domains. Q_L will be high if the FRET acceptor and the fluorescent protein are partitioned into the same domains, and Q_L will be low if the FRET acceptor and fluorescent protein are in different domains. Q_L depends not only on the partition of the FRET acceptor and the protein between the domains but also on the amount of each type of domain in the membrane. Since we do not know this information, we compare the results for PFO with results to standard proteins that are markers for Ld and Lo domains. The first standard protein is LW peptide, an alpha-helical peptide, which we have shown using independent measurements associates with Ld lipids, and has little raft affinity [65]. The second stand protein is cholera toxin B subunit (CT-B), which binds to the raft lipid ganglioside GM1, and localizes to lipid rafts (reviewed in [56]). We compared the behavior of these standard proteins, to two forms of PFO: WT PFO, which forms a TM beta-barrel in the membrane, and MUT PFO, a mutant which does not form the TM structure.

We also used two different FRET acceptors, pyrene-dioleoylphosphatidylethanolamine (pyrene-DOPE) a probe with unsaturated acyl chains

and thus disordered domain (Ld) affinity, and long chain TMA DPH (LcTMADPH), a derivative of DPH attached to a trimethyl-amino-terminated C22:0 hydrocarbon chain, which has ordered domains (Lo) affinity [35, 40, 127], to measure FRET. Figure 4.2 shows the structures of these probes.

Once we measure FRET between the proteins (LW, CT-B, and PFO) and the different energy acceptors, we can calculate a Q_L value for pyrene-DOPE and a Q_L value for LcTMADPH. In order to compare the overall behavior and affinity of proteins for the Ld or Lo FRET acceptors, we next calculate the ratio:

$$Q_L \text{ pyrene-DOPE} / Q_L \text{ LcTMADPH}$$

Comparing this ratio instead of the individual Q_L values for each FRET acceptor eliminates any parameters affected by changes within the protein that could change the protein's "quenchability" in one lipid environment (Ld membranes) compared to a different environment (Lo+Ld membranes). These changes would affect both FRET acceptors, so by taking the ratios of the Q_L values for each acceptor, we can directly compare the behavior of each protein..

Table 4.1 shows an example of the F/Fo ratios measured in both uniformly Ld membranes (composed of dioleoylphosphatidylcholine (DOPC) and cholesterol in a 6:4 ratio) and in membranes containing a ternary lipid mixture forming co-existing Ld and Lo domains (sphingomyelin (SM), DOPC, and cholesterol (3:3:4)). The latter lipid mixture is an approximate estimation of the outer leaflet of mammalian plasma membranes, and PFO forms SDS-resistant oligomers and pores vesicles with this composition (data not shown). The first column of Table 4.1 shows, for LW peptide and

the FRET acceptor pyrene-DOPE, a high amount of FRET (low F/Fo) in homogeneous membranes, and an increase in the amount of FRET in membranes containing Lo and Ld domains, indicating more pyrene-DOPE is close to the LW peptide (in the same domain) in the ternary lipid (Lo+Ld) lipid mixture. Conversely, for LcTMADPH, there is a decrease in the amount of FRET (higher F/Fo) in membranes containing Lo and Ld membranes compared to homogenous membranes, indicating a separation between LW peptide and the Lo domain FRET acceptor LcTMADPH (i.e. they are in different domains). The second column in Table 4.1 shows the F/Fo values for cholera toxin B (CT-B). Using pyrene-DOPE as the FRET acceptor, there is a decrease in the amount of FRET in comparing SM/DOPC/cholesterol to DOPC/cholesterol, indicating CT-B and pyrene-DOPE are in different domains in the the ternary lipid mixtures. Conversely, using LcTMADPH as a FRET acceptor, there is an increase in FRET in the Lo and Ld membranes compared to the homogeneous membranes, indicating they are in the same domain. It should be noted that we do think there may be complications in using LcTMADPH as an Lo FRET acceptor (see Discussion section). Due to this complication, instead of describing the changes seen within each F/Fo value for the WT and MUT PFO, we will focus on the Q_L values calculated for PFO and compare them to the Q_L values obtained for the standard proteins LW peptide and CT-B, through an additional calculation (described below).

In order to compare the behavior of PFO to CT-B and LW peptide to assess its affinity for ordered domains, we first calculated the Q_L values for pyrene-DOPE and LcTMADPH for LW peptide, CT-B, WT PFO, and MUT PFO (Table 4.2, first two rows). LW peptide has a high Q_L value for pyrene indicating an increase in local pyrene concentration surrounding the peptide, indicative of localization to the same domains (Ld). Conversely, it has a low Q_L value for LcTMADPH due to a decrease in local

LcTMADPH concentration surrounding the peptide, indicative of a separation of peptide and LcTMDPH into different domains. Cholera toxin B, however, has a Q_L value for pyrene-DOPE slightly higher than 1, indicating little change in the local concentration of pyrene-DOPE surrounding CT-B. CT-B has a Q_L for LcTMADPH around 1, also indicating little change in the local concentration of LcTMADPH. However, this value is higher than that of LW peptide which indicates more LcTMADPH is interacting with CT-B than LW peptide.

Next we calculated the Q_LPyrene/ Q_LLcTMADPH values for all proteins (Table 4.2, third row, in bold). LW peptide has a high Q_LPyrene/ Q_LLcTMADPH value, which is what would be expected if it partitioned in Ld domains. CT-B has a Q_LPyrene/ Q_LLcTMADPH much lower than LW peptide. WT PFO has a Q_LPyrene/ Q_LLcTMADPH value in between that of CT-B and LW peptide, indicating it has intermediate affinity for ordered domains. MUT PFO, however, has a Q_LPyrene/ Q_LLcTMADPH value that is slightly lower than CT-B, indicating that it associates strongly with ordered domains.

PFO associates with cholesterol-rich DRMs in model membranes

Since PFO has been shown to localize to detergent resistant membranes (DRMs) in cellular studies [86], we first measured PFO localization to DRMs by solubilizing BODIPY-labeled PFO-bound vesicles composed of SM/DOPC/chol (3:3:4) with Triton-X-100 (TX-100). It was necessary for PFO to be labeled with BODIPY because PFO location within each sucrose fraction was measured by fluorescence, and we found the signal of Trp alone was not sufficient over background measurements, since TX-100 has fluorescent properties which overlap with Trp. BODIPY fluorescence is measured at a

much higher wavelength and so its background measurements were less sensitive to the presence of TX-100. Figure 4.3A shows the lipid profile associated with detergent solubilization. The detergent insoluble material floats to the top of the gradient. As expected, the top two lightest fractions (fractions 1 and 2) contained high amounts of sphingomyelin (red) and cholesterol (blue), and low amounts of DOPC (purple). PFO (Figure 4.3B, red curve) primarily associated with fraction 2 of the sucrose gradient, corresponding to the fraction which contains the highest amount of SM and cholesterol (Figure 4.3A, red and blue). A control experiment, in which PFO was bound to DOPC/ cholesterol (3:2) vesicles and solubilized with TX-100 failed to show any PFO in the upper sucrose gradient fractions (data not shown). An additional control sample, also shown in Figure 4.3B (blue, dashed line), shows the non-specific interaction of PFO with DRMs when PFO is pre-bound to detergent-solubilized vesicles containing DOPC and cholesterol, and then mixed with detergent solubilized vesicles containing ordered domains (SM/DOPC/chol 3:3:4). Very little PFO appeared in fraction 2 in the control sample, which shows little transfer of PFO to DRMs after TX-100 was added. It should be be noted that DRM analysis was not able to be performed on the pre-pore MUT PFO without generating artifactual DRM association (see Discussion).

We also measured the localization of the FRET probes within DRMs. Figure 4.3C shows their sucrose gradient profiles when incorporated into SM/DOPC/cholesterol (3:3:4) vesicles and solubilized with TX-100 (Figure 4.3C). In fractions 1 and 2, corresponding (in Figure 4.2A) to where SM and cholesterol localize, there is more LcTMADPH (Lo probe, blue) than pyrene-DOPE (Ld probe, red) in the first two fractions of the gradient. However, localization of the probes is more similar than we expected from FRET results. Better separation of these probes into different domains was observed in later studies (see below).

Effect of Ceramide on PFO raft affinity

Ceramide is a saturated sphingolipid which has a small polar headgroup, similar to cholesterol. Ceramide has been shown to displace cholesterol from ordered domains containing SM, forming cer-rich domains with SM [40, 128-130]. To see if ceramide also displaces PFO from ordered domains, we measured FRET in SM/CER/DOPC/chol (1.5:1.5:3:4), and the F/Fo values are shown in Table 4.3. Both LW peptide and CT-B give values similar to measured in SM/DOPC/chol.

In Table 4.4, comparing the Q_LPyrene/ Q_LLcTMADPH (third row) for both PFO proteins to the standard proteins, the value for WT PFO is in closer proximity to the value obtained for CT-B indicating WT PFO has an affinity for ordered domains. MUT PFO had a Q_LPyrene/ Q_LLcTMADPH even closer to CT-B, indicating more ordered domain affinity than WT PFO. Since the behavior of both WT and MUT PFO is more similar to CT-B than LW peptide, we conclude that PFO has ordered domain affinity in SM/CER/ DOPC/chol, and does not get displaced from cer-rich domains.

We also measured the DRM association of PFO in ceramide containing vesicles. Figure 4.4A shows the lipids present in DRMs in vesicles containing SM/CER/dopc/chol. As expected, cholesterol (blue) has nearly been eliminated from the top-most fractions of the sucrose gradients, and instead ceramide (green) and SM (red) are the predominant lipids present in DRMs, indicating a displacement of cholesterol by ceramide. Figure 4.4B however, suprisingly shows PFO (red) still strongly associated with DRMs, despite the lack of cholesterol. Figure 4.4C shows that the Ld FRET acceptor pyrene-DOPE (red) is no longer associated at all with DRMs, while LcTMADPH (blue) still shows a

strong association with ordered domains, showing that these probes have an enhanced selectivity in ceramide containing membranes.

Effect of Saturated Phospholipid on PFO raft affinity

The studies above show that PFO has an affinity for ordered domains containg sphingolipids. To see if the presence of sphingolipid was required for raft affinity, PFO raft affinity was measured in membranes in which ordered domains contained phospholipid with saturated acyl chains, distearoylphosphatidylcholine (DSPC), in place of sphingomyelin. Table 4.5 shows an example the F/Fo values obtained for FRET between either pyrene-DOPE or LcTMADPH and LW peptide, CT-B, or PFO WT or MUT. The behavior of LW peptide and CT-B follow nearly the same pattern for DSPC/ DOPC/chol as in SM/DOPC/chol (Table 4.1).

The calculated Q_LPyrene/ Q_LLcTMADPH values for all proteins are shown in Table 4.6. (third row, in bold). LW peptide gives a very high Q_LPyrene/ Q_LLcTMADPH value (higher than that observed in previous lipid mixtures), indicating that in DSPC/ DOPC/chol it has strong partitioning into Ld domains. CT-B has a Q_LPyrene/ Q_LLcTMADPH lower than 1 indicative of partitioning into Lo domains. In contrast to the sphingolipid mixtures studied previously, in DSPC/DOPC/chol, WT PFO has a Q_LPyrene/ Q_LLcTMADPH value that is significantly higher than CT-B, indicating PFO has less Lo affinity. Similarly, MUT PFO also has a higher Q_LPyrene/ Q_LLcTMADPH indicating it has less ordered domain affinity.

We next studied the detergent insoluble properties of vesicles composed of DSPC/ DOPC/chol. Figure 4.5A shows the cholesterol profile in DSPC/DOPC/chol (3:3:4) (in

red). Only around 30% of radiolabeled cholesterol was in the ordered domain fractions, which is about half that observed for SM/DOPC/chol (Figure 4.3A, red), indicating that there is less cholesterol in DSPC Lo domains. When we compared the amount of PFO DRM association (Figure 4.5B, red) compared to control (Figure 4.5, blue, dashed), we observed substantial transfer to DRMs. This makes it difficult to interpret the extent of PFO DRM association affected in this lipid mixture. Figure 4.5C shows that the location of the Ld probe pyrene-DOPE (red) and the Lo probe LcTMADPH (blue) in DSPC/ DOPC/chol. More LcTMADPH is observed in top fractions of the gradient compared to pyrene-DOPE, confirming their respective domain affinities.

Effect of Unsaturated Lipid of PFO Raft Affinity

The structure of the unsaturated lipids forming the Ld domains might also affect raft affinity. Next, we measured the effect of the unsaturated phospholipid dimyrisoleoylphosphatidylcholine (DMoPC) on PFO raft affinity using FRET. DMoPC has an acyl chain length of 14 carbon, compared to DOPC, which has an acyl chain length of 18 carbons. Table 4.7 shows the F/Fo values obtained from FRET between either pyrene-DOPE or LcTMADPH and LW peptide, CT-B, or PFO WT or MUT. The behavior of LW peptide and CT-B follow nearly the same pattern for the other three lipid mixtures studied.

Table 4.8 contains the calculated Q_LPyrene/ Q_LLcTMADPH values for DSPC/ DMoPC/chol. LW peptide has an extremely high Q_LPyrene/ Q_LLcTMADPH value, indicative of an even stronger partitioning into Ld domains in the presence of DMoPC. Conversely, CT-B has a very low Q_LPyrene/ Q_LLcTMADPH value indicating a strong preference for ordered domains. WT PFO, however, has a Q_LPyrene/ Q_LLcTMADPH in between that of LW and CT-B (similar to what was observed in SM/DOPC/chol mixtures

(Table 4.2)). MUT PFO however, has a Q_LPyrene/ Q_LLcTMADPH value that is closer to CT-B, indicating MUT PFO has ordered domain affinity in DSPC/DMoPC/chol.

Figure 4.6A shows the cholesterol concentration in DRMs composed of DSPC/ DMoPC/chol. The amounts of cholesterol in the upper fractions of the sucrose gradient was similar to that in DRM composed of DSPC/DOPC/chol (Figure 4.5A), indicating the partitioning of cholesterol within ordered domains was not affected by the presence of DMoPC. There was also some association of PFO to DRMs (Figure 4.6B, red), however there was still a large amount of transfer to DRMs after the addition of TX-100 (Figure 4.6B, blue, dashed), making it difficult to compare the difference in DRM association between DSPC/DMoPC/chol and DSPC/DOPC/chol. Figure 4.6C shows that the location of the Ld probe pyrene-DOPE (red) and the Lo probe LcTMADPH (blue) retain their respective partitioning properties in DSPC/DMoPC/chol.

Effect of Cholesterol Concentrations on Raft Affinity

We calculated how similar the behavior of WT and MUT was to CT-B and LW peptide. Table 4.9 shows a summary of the FRET results obtained from all four lipid mixture used to study raft affinity of PFO. A value of 100% for PFO would indicat that the Q_LPyrene/ Q_LLcTMADPH for PFO was equal to that of CT-B, and therefore has ordered domain affinity. A value of 0% for PFO would indicate that the Q_LPyrene/ Q_LLcTMADPH for PFO was equal to that of LW peptide, and therefore has no ordererd domain affinity.

In order to see if there was a correlation between the concentration of cholesterol within ordered domains and the raft affinity of PFO, we directly compared the amount of cholesterol within ordered domains to the amount of raft-associated PFO for each lipid

mixture. Table 4.9 also shows the percentage of radiolabeled cholesterol within DRMs (fractions 1, 2, and 3) compared to the percentage of PFO that behaves like CT-B for each lipid mixture. There does not seem to be a direct correlation to high cholesterol concentrations in ordered domains and PFO having more raft affinity for ordered domains in these mixtures.

DISCUSSION

Role of cholesterol in raft affinity of PFO

The proposed ability of PFO to bind to ordered domains in cells is believed to be driven by its affinity for cholesterol-rich ordered domains. One striking observation from this study was that PFO raft affinity was not affected solely by the concentration of cholesterol within ordered domains, since PFO raft association was high in both SM/ dopc/chol, where cholesterol concentrations were high, and in SM/CER/dopc/chol, where cholesterol concentrations were low (Table 4.9).

Formation of ordered domains is driven by the ability of the lipids within the domain to pack tightly. Cholesterol interacts more favorably and packs more tightly with saturated phospho- and sphingolipids than unsaturated phospholipids (reviewed in [131]). It is believed that ceramide displaces cholesterol from ordered domains because both lipids have small polar headgroups and in order to avoid exposure to the aqueous solvent surrounding the membrane, they compete for space underneath saturated phospholipids to shield themselves from water [40], in accordance with the umbrella model [39]. Based on this assumption, it seems as though ceramide should also displace PFO from ordered domains if sterol binding is what gives PFO its raft affinity. However, we observed strong raft association of PFO even in the presence of ceramide. This may be because PFO bound cholesterol is shielded from water, thereby preventing unfavorable exposure to water, and allowing it to pack tightly with SM and ceramide. This is illustrated in Figure 4.7.

The observation that PFO has less raft affinity in DSPC containing membranes may be due to a decrease in ability of cholesterol to pack within DSPC ordered domains.

DSPC has a higher TM than sphingomyelin, which means DSPC-DSPC interactions are strong, and may replace DSPC-sterol interactions. In agreement with this, our DRM analysis shows less cholesterol is associated in DSPC-rich ordered domains. Since cholesterol has a lower affinity for DSPC-ordered domains, and there is no reason that PFO binding might enhance this affinity, less PFO remains in rafts. Combined with the results from ceramide mixtures, the pattern of PFO raft affinity observed for this study supports a model in which PFO-bound cholesterol maintains it's ability to pack tightly in ordered domains, but does not enhance cholesterol's ability to pack in ordered domains in which cholesterol has a lower affinity.

While we did observe more raft affinity for PFO in DSPC/DMoPC/chol compared to DSPC/DOPC/chol, the interpretation of that result is less clear. This result can not be explained by free cholesterol location as we observed nearly equal amounts of cholesterol within DRMs for both lipid mixtures. It may be possible packing between DMoPC and PFO bound cholesterol is such that it disfavors PFO-bound cholesterol location in the Ld domains of DSPC/DMoPC/chol membranes, increasing its affinity for ordered domains for this lipid composition.

Role of beta-barrel formation in raft affinity of PFO.

The origin of how trans-membrane proteins interact with lipid rafts in not understood. We have shown previously that the sterol specificity of WT PFO does not differ from the non-TM PFO mutant (studied here [124]). Furthermore, it has been shown that domain 4 (the cholesterol binding domain of PFO) has the same affinity for cholesterol-rich membranes as the entire PFO molecule [85]. Therefore, any difference between the WT and MUT PFO raft affinity must only be attributed to formation of the beta-barrel and not to any differences in affinity of PFO for sterol-rich membranes. In all

lipid mixtures examined by FRET, the non-TM form of PFO had significantly more raft affinity than the WT TM form. This result demonstrates that, even over the average of all lipid conditions, formation of the beta-barrel by PFO reduces its affinity for ordered domains. Since both CT-B and MUT PFO are only peripherally associated with the membrane surface and binds lipids that tend to concentrate in rafts, it is not surprising that their raft affinities would be similar.

Why does the TM beta-barrel reduce raft affinity? Since FRET measures the local lipid environment surrounding fluorophores, the difference observed between the WT and MUT protein likely reflect local changes within membrane structure. TM segments of membrane proteins should pack poorly into ordered lipid domains, in which tight packing leads to strong lipid-lipid interactions. We postulate, then, that the transmembrane beta-barrel must cause PFO to localize to a more disordered lipid environment. How can this occur such that PFO remains raft associated? One way this could happen is that a small re-arrangement of disordered lipids surrounds the beta-barrel once it is formed, so that the inserted structure locally surrounded by Ld lipids (Figure 4.8A). Another model might be that the membrane inserted beta-barrel is associating primarily with raft edges (Figure 4.8B).

Issues concerning FRET analysis

We have proposed that the FRET analysis is more accurate when the quenching data for pyrene-DOPE and LcTMADAPH are combined. If we analyze the results from a single FRET acceptor, our FRET analysis with the Ld energy acceptor pyrene-DOPE has shown consistently in all lipid mixtures observed that PFO Lo affinity is between that of LW peptide and CT-B. This result agrees with our observation that PFO associates with DRMs more strongly in the lipid mixtures where the behavior of PFO more closely

resembles that of cholera toxin. The results from the LcTMADPH FRET assay by themselves been more ambiguous and difficult to interpret, and the origin of this difference between the two FRET acceptors is not clear.

Since our results for LcTMADPH do not correlate well to what we observe using pyrene-DOPE and DRM analysis , we believe it less reliable as a FRET acceptor as compared to pyrene-DOPE. Nevertheless, even if we use only the LcTMADPH FRET data it does not change the observation that the non-TM PFO mutant showed more raft affinity than the TM wild-type PFO. This trend is observed for both pyrene and LcTMADPH, with the only difference being LcTMADPH reporting more Ld affinity for both forms of PFO in all lipid mixtures.

Detergent Resistant Membrane Analysis

Our experiments show that transfer within DRMs can be a problem for proteins. It should be noted that when DRM association was examined with the "pre-pore" mutant of PFO, it was found to be in the top fractions of the sucrose gradients in every lipid mixture examined (data not shown). However, in the control experiments, we found that pre-pore MUT was associated with vesicles lacking ordered domains prior to detergent solubilization was bound to DRMs from vesicles containing ordered domains . We believe the origin of this behavior might stem from the detergent TX-100 stripping cholesterol from the surface of the bound PFO mutant. Since the mutant does not form the TM structure, the only association it has with the membrane is presumably through its cholesterol binding. When it falls of the membrane, it has no hydrophobic surfaces exposed so it should not be associated with detergent micelles. If detergent resistant membranes are present in which there is sufficient cholesterol concentrations, PFO could rebind to these DRMs and so be DRM-associated after sucrose gradient analysis. In

accordance with this hypothesis, we found no transfer contamination when DRMs lacked sufficient cholesterol concentrations for MUT PFO membrane association (data not shown). This artifact requires further characterization, but it does place constraints on cellular studies which seek to use non-TM forming PFO, or its isolated membrane binding domain for lipid raft DRM localization [85, 86].

It should also be noted that this artifact was also observed for the WT PFO (as mentioned), although not in every case, or to as high an extent as in the pre-pore samples. This contamination indicates that detergent-solubilized PFO sticks to cholesterol-rich DRMs in which it was not previously associated to some degree. In any case, DRM results for the purpose of this study were used to confirm the observations from FRET analysis and did not use it as a quantitative measurement for the extent of PFO raft association. However, this could be a problem if studying TM protein DRM association in cells.

Table 4.1. F/Fo ratios for lipid mixtures of uniform Ld membranes (DOPC/CHOL 6:4) and Lo and Ld membranes (SM/DOPC/CHOL 3:3:4) for LW peptide, cholera toxin B subunit (CT-B), wild-type (WT) and mutant (MUT) PFO for the Ld FRET acceptor pyrene-DOPE and the Lo FRET acceptor LcTMADPH. Values given show the average F/Fo and standard deviation obtained from three separate samples from one experiment, each of which had 3 samples.

FRET ACCEPTOR	LIPID MIXTURE	LW PEPTIDE	CT-B	WT PFO	MUT PFO
pyrene-DOPE	DOPC/CHOL (6:4)	.160 ± .002	.504 ± .033	.335 ± .023	.353 ± .014
pyrene-DOPE	SM/DOPC/CHOL (3:3:4)	.065 ± .001	.541 ± .081	.335 ± .017	.393 ± .009
LcTMADPH	DOPC/CHOL (6:4)	.337 ± .006	.549 ± .044	.323 ± .019	.267 ± .011
LcTMADPH	SM/DOPC/CHOL (3:3:4)	.395 ± .006	.538 ± .084	.482 ± .028	.339 ± .042

Table 4.2. Q_L and Q_L pyrene-DOPE/ Q_L LcTMADPH values measured for vesicles with lipid composition SM/DOPC/CHOL (3:3:4) for LW peptide, cholera toxin B, wild-type, and mutant PFO. Values shown are the averages and standard deviations from 3 separate experiments, each of which had 3 samples. The value of Q_L pyrene-DOPE/ Q_L LcTMADPH is shown in the final row (Q_LPyr/Q_LLc**)**. The higher the Q_LPyr/Q_LLc value, the lower the raft affinity.

FRET ACCEPTOR	LIPID MIXTURE	LW PEPTIDE	CT-B	WT PFO	MUT PFO
pyrene-DOPE	SM/DOPC/CHOL (3:3:4)	1.537 ± .106	1.008± .179	1.079± .089	.857 ± .052
LcTMADPH	SM/DOPC/CHOL (3:3:4)	.809 ± .133	.971 ± .080	.782 ± .088	.845 ± .039
Q_LPyr/Q_LLc	**SM/DOPC/CHOL (3:3:4)**	**1.901±.339**	**1.038±.204**	**1.450±.209**	**1.015±.077**

Table 4.3. F/Fo ratios for lipid mixtures of uniform Ld membranes (DOPC/CHOL 6:4) and Lo and Ld membranes (SM/CER/DOPC/CHOL 1.5:1.5:3:4) for LW peptide, cholera toxin B subunit (CT-B), wild-type (WT) and mutant (MUT) PFO for the Ld FRET acceptor pyrene-DOPE and the Lo FRET acceptor LcTMADPH. Values given show the average F/Fo and standard deviation obtained from three separate samples from one experiment, each of which had 3 samples.

FRET ACCEPTOR	LIPID MIXTURE	LW PEPTIDE	CT-B	WT PFO	MUT PFO
pyrene-DOPE	DOPC/CHOL (6:4)	.167 ± .010	.517 ± .016	.361 ± .019	.356 ± .012
pyrene-DOPE	SM/CER/DOPC/ CHOL (1.5:1.5:3:4)	.075 ± .002	.531 ± .038	.344 ± .007	.400 ± .045
LcTMADPH	DOPC/CHOL (6:4)	.301 ± .015	.514 ± .021	.297 ± .018	.229 ± .015
LcTMADPH	SM/CER/DOPC/ CHOL (1.5:1.5:3:4)	.391 ± .016	.524 ± .050	.288 ± .010	.273 ± .007

Table 4.4. Q_L values for both pyrene-DOPE and LcTMADPH measured for vesicles with lipid composition SM/CER/DOPC/CHOL (1.5:1.5:3:4) for LW peptide, cholera toxin B, wild-type, and mutant PFO. Values shown are the averages and standard deviations from 3 separate experiments, each of which had 3 samples. The value of Q_L pyrene-DOPE/ Q_L LcTMADPH is shown in the final row (Q_LPyr/Q_LLc**)**. The higher the Q_LPyr/Q_LLc value, the lower the raft affinity.

FRET ACCEPTOR	LIPID MIXTURE	LW PEPTIDE	CT-B	WT PFO	MUT PFO
Q_L pyrene-DOPE	SM/CER/DOPC/ CHOL (1.5:1.5:3:4)	1.541± .174	.948 ± .082	.958± .120	.868 ± .030
Q_L LcTMADPH	SM/CER/DOPC/ CHOL (1.5:1.5:3:4)	.694 ± .081	1.008±.189	.774 ± .285	.783 ± .129
Q_LPyr/Q_LLc	**SM/CER/DOPC/ CHOL (1.5:1.5:3:4)**	**2.222 ±.360**	**.940 ±.194**	**1.238 ±.483**	**1.109 ±.186**

Table 4.5. F/Fo ratios for lipid mixtures of uniform Ld membranes (DOPC/CHOL 6:4) and Lo and Ld membranes (DSPC/DOPC/CHOL 3:3:4) for LW peptide, cholera toxin B subunit (CT-B), wild-type (WT) and mutant (MUT) PFO for the Ld FRET acceptor pyrene-DOPE and the Lo FRET acceptor LcTMADPH. Values given show the average F/Fo and standard deviation obtained from three separate samples from one experiment, each of which had 3 samples.

FRET ACCEPTOR	LIPID MIXTURE	LW PEPTIDE	CT-B	WT PFO	MUT PFO
pyrene-DOPE	DOPC/CHOL (6:4)	.160 ± .002	.504 ± .033	.335 ± .023	.353 ± .014
pyrene-DOPE	DSPC/DOPC/ CHOL (3:3:4)	.061 ± .001	.602 ± .049	.269 ± .026	.295 ± .033
LcTMADPH	DOPC/CHOL (6:4)	.337 ± .006	.549 ± .044	.323 ± .019	.267 ± .011
LcTMADPH	DSPC/DOPC/ CHOL (3:3:4)	.549 ± .013	.546 ± .020	.587 ± .047	.445 ± .051

Table 4.6. Q_L values for both pyrene-DOPE and LcTMADPH measured for vesicles with lipid composition DSPC/DOPC/CHOL (3:3:4) for LW peptide, cholera toxin B, wild-type, and mutant PFO. Values shown are the averages and standard deviations from 2 separate experiments, each of which had 3 samples. The value of Q_L pyrene-DOPE/ Q_L LcTMADPH is shown in the final row (Q_LPyr/Q_LLc**)**. The higher the Q_LPyr/Q_LLc value, the lower the raft affinity.

FRET ACCEPTOR	LIPID MIXTURE	LW PEPTIDE	CT-B	WT PFO	MUT PFO
pyrene-DOPE	DSPC/DOPC/ CHOL (3:3:4)	1.549 ± 033	.883 ± .179	1.263± .089	1.178 ± .006
LcTMADPH	DSPC/DOPC/ CHOL (3:3:4)	.618 ± .093	.989 ± .027	.546 ± .105	.589 ± .013
Q_LPyr/Q_LLc	**DSPC/ DOPC/CHOL (3:3:4)**	**2.506 ±.380**	**.893 ±.205**	**2.313 ±.474**	**2.008 ±.45**

Table 4.7. F/Fo ratios for lipid mixtures of uniform Ld membranes (DMoPC/CHOL 6:4) and Lo and Ld membranes (DSPC/DMoPC/CHOL 3:3:4) for LW peptide, cholera toxin B subunit (CT-B), wild-type (WT) and mutant (MUT) PFO for the Ld FRET acceptor pyrene-DOPE and the Lo FRET acceptor LcTMADPH. Values given show the average F/Fo and standard deviation obtained from three separate samples from one experiment, each of which had 3 samples.

FRET ACCEPTOR	LIPID MIXTURE	LW PEPTIDE	CT-B	WT PFO	MUT PFO
pyrene-DOPE	DMoPC/CHOL (6:4)	.164 ± .005	.512 ± .019	.285 ± .005	.322 ± .009
pyrene-DOPE	DSPC/DMoPC/ CHOL (3:3:4)	.055 ± .002	.622 ± .026	.286 ± .011	.414 ± .036
LcTMADPH	DMoPC/CHOL (6:4)	.268 ± .009	.540 ± .015	.226 ± .005	.191 ± .007
LcTMADPH	DSPC/DMoPC/ CHOL (3:3:4)	.587 ± .018	.513 ± .024	.485 ± .024	.390 ± .033

Table 4.8. Q_L values for both pyrene-DOPE and LcTMADPH measured for vesicles with lipid composition DSPC/DMoPC/CHOL (3:3:4) for LW peptide, cholera toxin B, wild-type, and mutant PFO. Values shown are the averages and standard deviations from 2 separate experiments, each of which had 3 samples. The value of Q_L pyrene-DOPE/ Q_L LcTMADPH is shown in the final row (Q_LPyr/Q_LLc**)**. The higher the Q_LPyr/Q_LLc value, the lower the raft affinity.

FRET ACCEPTOR	LIPID MIXTURE	LW PEPTIDE	CT-B	WT PFO	MUT PFO
pyrene-DOPE	DSPC/DMoPC/ CHOL (3:3:4)	1.569 ±.049	.703 ± .009	.985 ± .018	.775 ± .004
LcTMADPH	DSPC/DMoPC/ CHOL (3:3:4)	.420 ± .022	1.042 ± .059	.453 ± .048	.548 ± .017
Q_LPyr/Q_LLc	**DSPC/DMoPC/ CHOL (3:3:4)**	**3.740 ±.568**	**.675 ±.039**	**2.174 ±.233**	**1.414 ±.05**

Table 4.9. CT-B or LW peptide-like behavior of wild-type and mutant PFO. Values obtained by comparing the Q_L values for both pyrene-DOPE and LcTMADPH and averaging the difference in behavior of PFO with that of LW peptide. The % of ^{3}H-chol found in the top 3 fractions of sucrose gradients for each lipid mixtures is also shown in the final column.

LIPID MIXTURE	LW PEPTIDE	CT-B	WT PFO	MUT PFO	% cholesterol in DRMs
SM/DOPC/CHOL (3:3:4)	0%	100%	52%	>100%	**66**
SM/CER/DOPC/ CHOL (1.5:1.5:3:4)	0%	100%	77%	87%	**11**
DSPC/DOPC/CHOL (3:3:4)	0%	100%	12%	31%	**30**
DSPC/DMoPC/ CHOL (3:3:4)	0%	100%	51%	76%	**25**

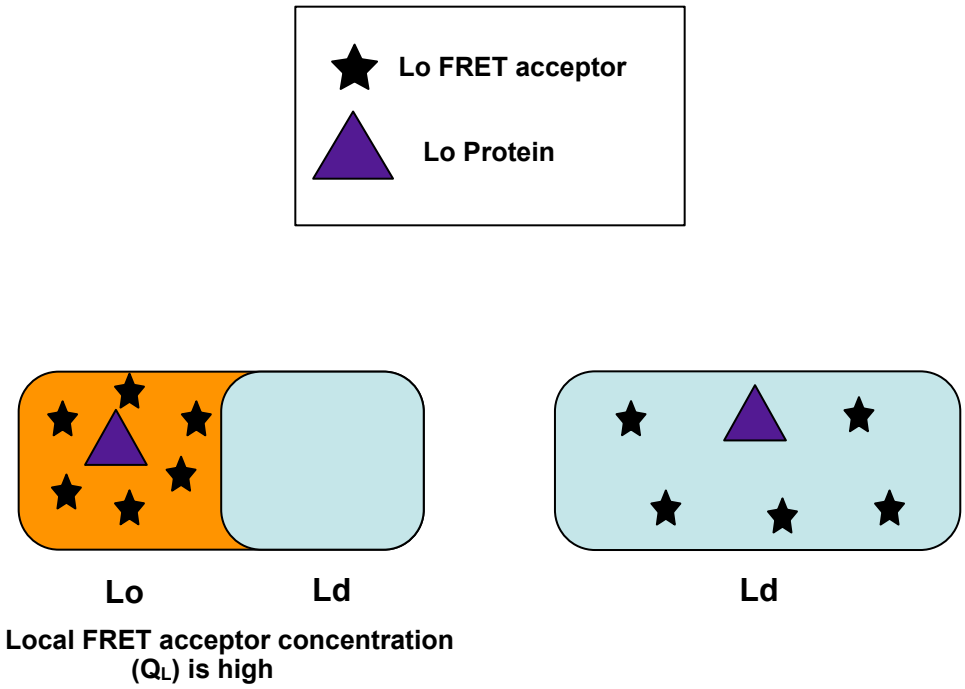

Figure 4.1: Schematic diagram of local FRET acceptor concentration (Q_L). In membranes containing mixtures of Lo and Ld domains (orange and blue, respectively), a protein with Lo affinity will have a high Q_L value because the Lo FRET acceptor is more concentrated within ordered domains as compared to the uniform Ld membranes.

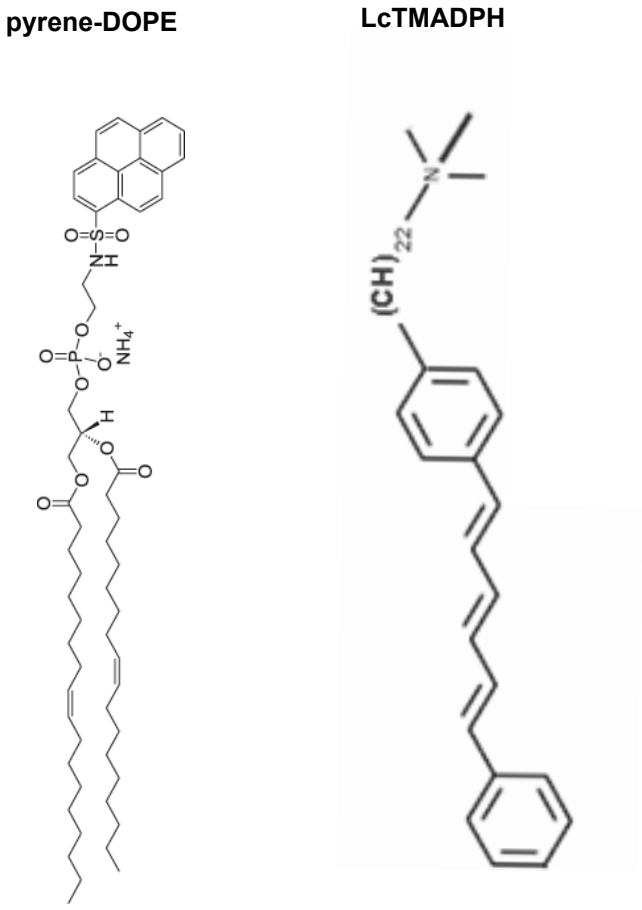

Figure 4.2: Structures of FRET acceptors used for raft affinity assay. pyrene-DOPE partitions into Ld domains, LcTMADPH partitions into Lo domains.

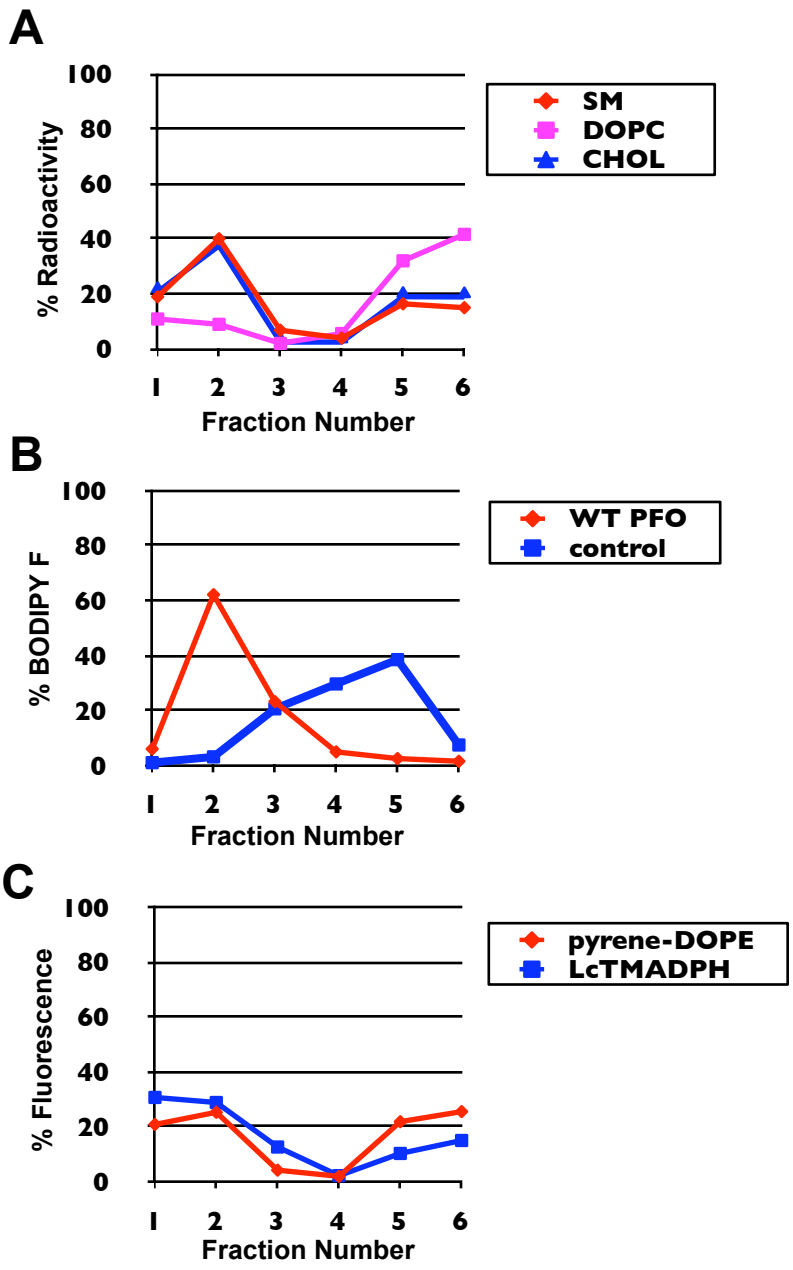

Figure 4.3: DRM analysis for SM/DOPC/chol (3:3:4). Fraction 1 indicates the top (and least dense) sucrose gradient fraction. (A) Lipid composition within DRMs, as measured by radioactivity in each fraction (B) WT PFO association with DRMs as measured by the fluorescence intensity of BODIPY labeled PFO. Control indicates association of PFO associated with DRMs when bound to non-DRM containing vesicles. (C) FRET acceptor association with DRMs, as measured by fluorescence. For (A) and (B, blue curve) in this and all remaining DRM figures, results shown are the averages of at least 4 samples run on at least 2 different days. For (B, red curve) and (C), results shown are averages of duplicates samples prepared on the same day.

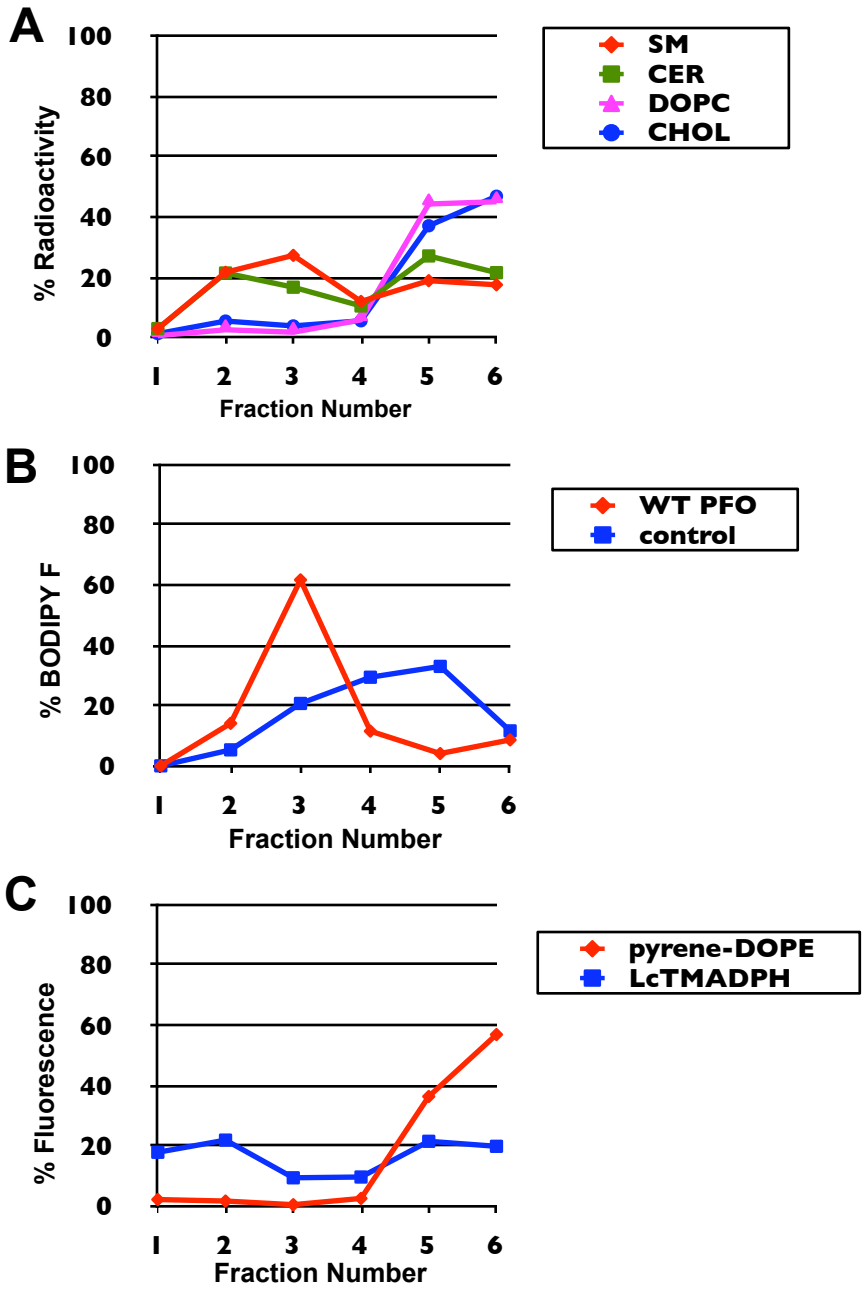

Figure 4.4: DRM analysis for SM/CER/DOPC/chol (1.5:1.5:3:4). Fraction 1 indicates the top (and least dense) sucrose gradient fraction. (A) Lipid composition within DRMs, as measured by radioactivity in each fraction (B) WT PFO association with DRMs as measured by the fluorescence intensity of BODIPY labeled PFO in each fraction. Control indicates association of PFO associated with DRMs when bound to non-DRM containing vesicles (C) FRET acceptor association with DRMs, as measured by fluorescence.

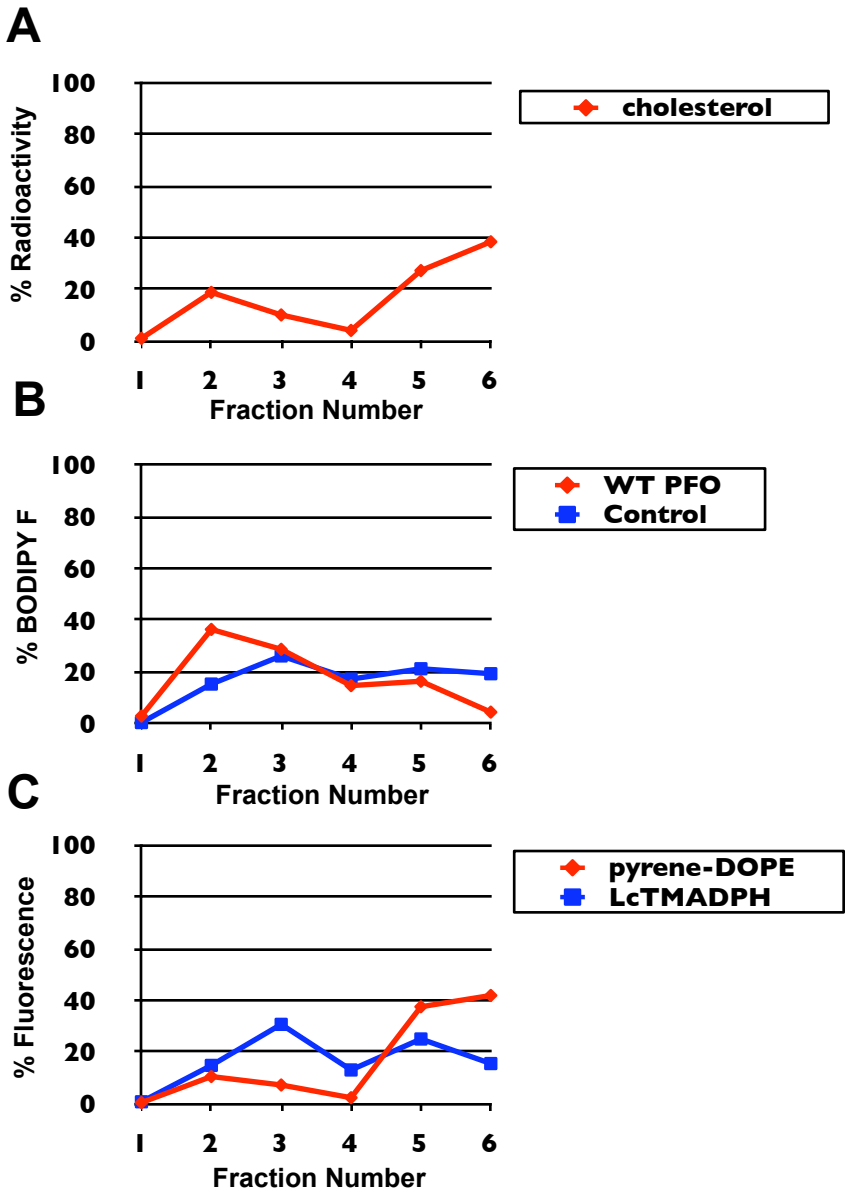

Figure 4.5: DRM analysis for DSPC/DOPC/chol (3:3:4). Fraction 1 indicates the top (and least dense) sucrose gradient fraction. (A) Cholesterol composition within DRMs, as measured by radioactivity in each fraction (B) WT PFO association with DRMs as measured by the fluorescence intensity of BODIPY labeled PFO in each fraction. Control indicates association of PFO associated with DRMs when bound to non-DRM containing vesicles. (C) FRET acceptor association with DRMs, as measured by fluorescence.

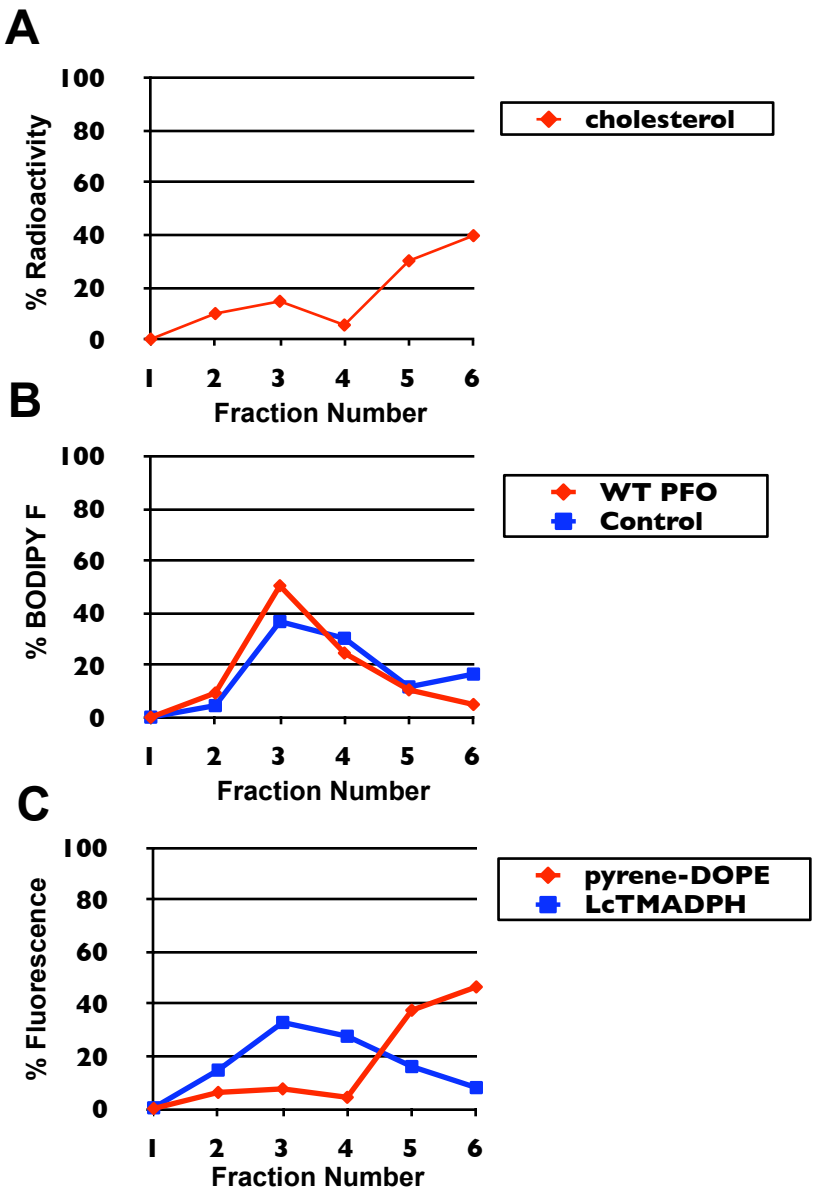

Figure 4.6: DRM analysis for DSPC/DMoPC/chol (3:3:4). Fraction 1 indicates the top (and least dense) sucrose gradient fraction. (A) Cholesterol composition within DRMs, as measured by radioactivity in each fraction (B) WT PFO association with DRMs as measured by the fluorescence intensity of BODIPY labeled PFO in each fraction. Control indicates association of PFO associated with DRMs when bound to non-DRM containing vesicles. (C) FRET acceptor association with DRMs, as measured by fluorescence.

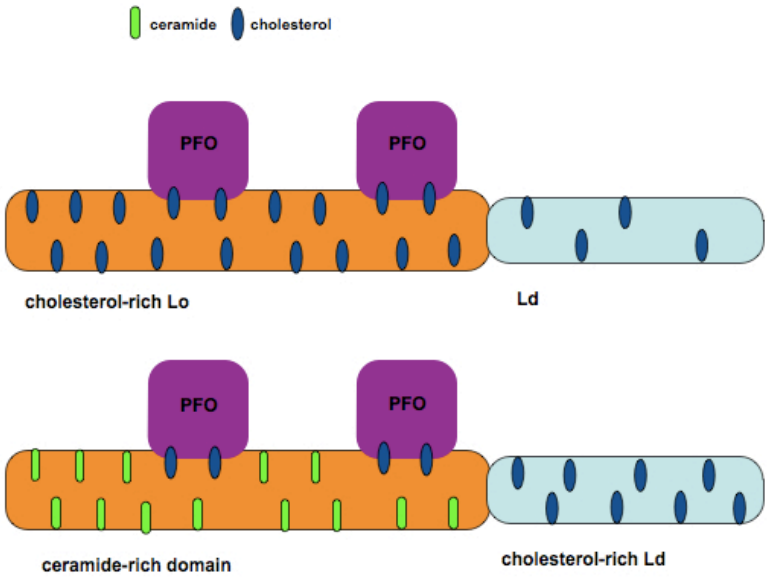

Figure 4.7: Schematic diagram of PFO association with cer-rich domains. In top panel, ordered domains are enriched in cholesterol which promotes PFO raft association. In bottom panel, the presence of ceramide displaces cholesterol from ordered domains. PFO binding to cholesterol allows it to pack within ceramide-rich domains.

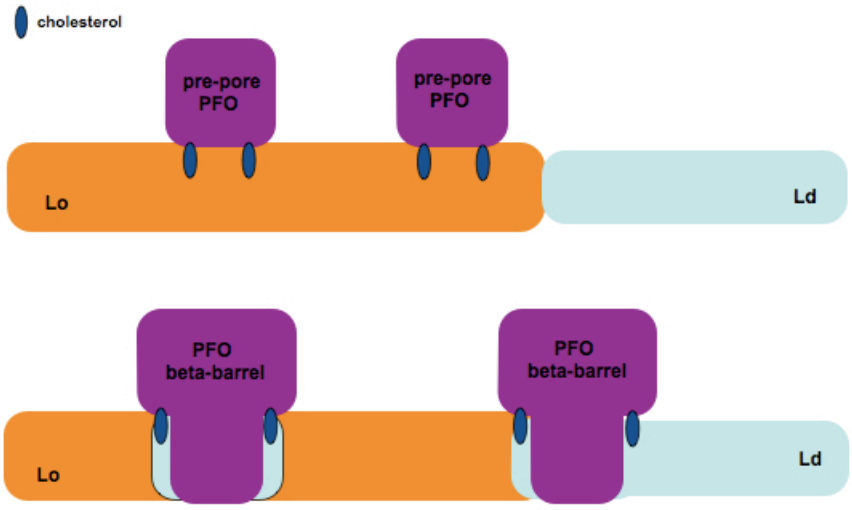

Figure 4.8: Schematic diagram of pre-pore vs. beta barrel PFO raft affinity. In top panel pre-pore PFO associates with cholesterol-rich ordered domains (cholesterol not shown for simplification). In bottom panel, the beta-barrel formed by PFO is still associated with ordered domains, but more locally associated with Ld lipids (light blue).

CHAPTER 5

Summary and Future Directions

SUMMARY

Over the course of this thesis project, we have examined how aqueous environment, phospholipid structure, and sterol structure affect how the cholesterol dependent cytolysin perfringolyin O associates with model membranes. We have also measured how these same parameters control the affinity of PFO for ordered domains (lipid rafts). Since PFO is a transmembrane (TM) protein, studying the PFO-ordered domain interaction is of interest because it is not well understood how TM proteins associate with lipid rafts.

One of the first observations we made was that low pH triggers PFO binding, oligomerization, and insertion at lower cholesterol concentrations compared to neutral pH. Prior to this discovery it had generally been assumed that PFO forms pores in plasma membranes [90] . Combined with the recent evidence the PFO is required for escape within host macrophages [91], it is now a very likely possibility that PFO functions at both neutral and low pH *in vivo*.

We also studied the ability of PFO to bind to different sterols. Our lab had previously shown that certain sterols such as dihydrocholesterol and lathosterol promote formation of ordered domains similar to cholesterol, while other sterols inhibit ordered domain formation (such as coprostanol) [35-38]. Since PFO is believed to bind to lipid rafts, I investigated the ability of PFO to recognize raft and non-raft sterols within binary lipid membranes, and found no correlation between the raft-promoting ability of the sterol and its ability to be recognized by PFO. Interestingly, although PFO bound to diverse sterol with various affinities, there was with no difference in the dependence of binding affinity upon sterol structure between the wild-type, pore-forming protein, and a

mutant which is trapped in the "pre-pore" state. This indicates formation of the beta-barrel by PFO does not affect sterol specificity. We also investigated the ability of PFO to bind to binary mixtures of different phospholipids and cholesterol. PFO interactions with sterol were inversely related to the packing properties of the phospholipids. Specifically, the looser the packing of the phospholipids**,** the lower the concentration of cholesterol needed to induce insertion of PFO into the lipid bilayer. Similarly, lipids with small headgroups (such as ceramide) were found to enhance PFO binding to membranes. This behavior can be explained in terms of the effect of loose packing upon cholesterol chemical reactivity. Acyl chain and headgroup structures that limit the ability of cholesterol to pack closely with phospholipids should limit this shielding of cholesterol from water, thereby increasing cholesterol reactivity and thus its tendency to bind to other molecules [39]. Combined, these observations are consistent with a model in which the strength and specificity of sterol interaction arises from both sterol interactions with domain 4 and sterol chemical activity within membranes.

The above studies were essential in order to develop a system to study lipid raft affinity in model membranes. In order to study PFO in its membrane-inserted, TM state, PFO must first recognize membrane cholesterol and form oligomers. This process has been shown to require high concentrations of sterol, with many model membrane studies requiring 50 mol% cholesterol within vesicles in order for PFO to form pores [94]. Understanding the factors which promote PFO membrane association, most importantly that low pH reduces the amount of cholesterol needed for PFO pore formation, allowed us to use many more lipid conditions to study raft affinity than we originally thought possible at the beginning of this project.

Finally, we examined lipid raft affinity in model membranes using both fluorescence resonance energy transfer (FRET) and detergent-resistant membranes (DRMs). We confirmed that, in vesicles mimicking the outer leaflet of the plasma membrane, PFO does indeed partition into ordered domains in both the TM and non-TM (pre-pore) state, although not to as high a degree as the raft marker cholera toxin B. This was also true in several different lipid mixtures containing co-existing ordered and Ld domains. However, in every case PFO raft affinity was reduced in the TM state. In addition, PFO raft association was not correlated to the amount of cholesterol within ordered domains. The presence of ceramide, which displaced cholesterol from ordered domains, did not displace PFO. Combined, these studies have suggested a model for PFO raft affinity that is not solely dependent upon cholesterol concentrations within ordered domains, but also upon the ability of the complex of PFO and bound cholesterol to pack favorably into ordered domains.

FUTURE DIRECTIONS

Measuring Raft Affinity of PFO in GUVs

Giant unilamellar vesicles (GUVs) are large micron size model membrane vesicles which are visible using fluorescent or confocal microscopy, and have been frequently used to observe phase co-existence in different binary and ternary mixtures of lipids (recently reviewed in [132, 133]). Since we have already optimized the conditions for studying raft affinity in model membranes, it seems an obvious next step to visualize PFO co-localization to lipid rafts using GUV fluorescence microscopy, and compare the results to those obtained through my previous spectroscopic analysis, in order to confirm raft affinity by an independent method. One idea is to see if the difference between wild-type pore-forming PFO and the non-TM pre-pore mutant have different lipid raft affinities that can be visualized microscopically. If the difference in raft affinity between the WT and non-TM form of PFO is due to local lipid environment, measuring raft affinity microscopically would report higher raft affinity of the TM form of PFO than our spectroscopic assay.

Effect of Oligomerization on PFO Raft Affinity

Another idea is to measure how oligomerization affects the affinity of PFO for ordered domains. Both the WT and pre-pore mutant I have studied previously form oligomeric complexes, and it has been shown in cells that another cholesterol dependent cytolysin aggregates lipid rafts by oligomerization [83]. Studying the raft localization of only the membrane binding domain of PFO would determine if oligomerization was necessary for PFO raft association in different lipid mixtures.

Effect of Cholesterol Depletion and Sterol Substitution on PFO Raft Affinity

We have identified both lipid raft-promoting and raft-inhibiting sterols that PFO is able to bind to in model membranes. In order to directly test if PFO binding to sterol would affect its association with lipid rafts, it would be ideal to see if PFO binding to non-raft forming sterols would inhibit PFO raft association. Unfortunately, formation of the TM structure of PFO requires that high amounts of non-raft forming sterols be present within membranes. At these high non-raft sterol concentrations, it is nearly impossible to make model membrane vesicles that contain domains in the Lo state.

An alternative method would be to first allow TM formation of PFO within cholesterol-rich model membrane vesicles. Once fully inserted, methyl-beta-cyclodextrin could be used to entirely extract cholesterol from the membrane. After all the cholesterol has been depleted, sterols with various lipid raft promoting properties could be re-introduced into the bilayer, and the effect of these sterols on PFO lipid raft association could be measured.

Studying PFO Association with Asymmetric Vesicles

Our lab has recently developed a method to make asymmetric large and small unilamellar vesicles [51]. Since these vesicles more closely mimic mammalian cellular membranes, it would be exciting to see how PFO cholesterol binding, oligomerization, pore-formation, and lipid raft binding properties change in asymmetric membranes compared to symmetric membranes.

REFERENCES

1. Lafont, F. and F.G. van der Goot, *Bacterial invasion via lipid rafts.* Cell Microbiol, 2005. **7**(5): p. 613-20.
2. Simons, K. and D. Toomre, *Lipid rafts and signal transduction.* Nat Rev Mol Cell Biol, 2000. **1**(1): p. 31-9.
3. Conner, S.D. and S.L. Schmid, *Regulated portals of entry into the cell.* Nature, 2003. **422**(6927): p. 37-44.
4. Parton, R.G. and A.A. Richards, *Lipid rafts and caveolae as portals for endocytosis: new insights and common mechanisms.* Traffic, 2003. **4**(11): p. 724-38.
5. Deans, J.P., H. Li, and M.J. Polyak, *CD20-mediated apoptosis: signalling through lipid rafts.* Immunology, 2002. **107**(2): p. 176-82.
6. Campbell, S.M., S.M. Crowe, and J. Mak, *Lipid rafts and HIV-1: from viral entry to assembly of progeny virions.* J Clin Virol, 2001. **22**(3): p. 217-27.
7. Ahn, A., D.L. Gibbons, and M. Kielian, *The fusion peptide of Semliki Forest virus associates with sterol-rich membrane domains.* J Virol, 2002. **76**(7): p. 3267-75.
8. Ipsen, J.H., et al., *Phase equilibria in the phosphatidylcholine-cholesterol system.* Biochim Biophys Acta, 1987. **905**(1): p. 162-72.
9. Almeida, P.F., W.L. Vaz, and T.E. Thompson, *Lateral diffusion in the liquid phases of dimyristoylphosphatidylcholine/cholesterol lipid bilayers: a free volume analysis.* Biochemistry, 1992. **31**(29): p. 6739-47.
10. Rubenstein, J.L., B.A. Smith, and H.M. McConnell, *Lateral diffusion in binary mixtures of cholesterol and phosphatidylcholines.* Proc Natl Acad Sci U S A, 1979. **76**(1): p. 15-8.
11. Lee, A.G., *Lipid phase transitions and phase diagrams. II. Mictures involving lipids.* Biochim Biophys Acta, 1977. **472**(3-4): p. 285-344.
12. Samsonov, A.V., I. Mihalyov, and F.S. Cohen, *Characterization of cholesterol-sphingomyelin domains and their dynamics in bilayer membranes.* Biophys J, 2001. **81**(3): p. 1486-500.
13. Kahya, N., et al., *Probing lipid mobility of raft-exhibiting model membranes by fluorescence correlation spectroscopy.* J Biol Chem, 2003. **278**(30): p. 28109-15.
14. Dietrich, C., et al., *Lipid rafts reconstituted in model membranes.* Biophys J, 2001. **80**(3): p. 1417-28.
15. Veatch, S.L. and S.L. Keller, *Miscibility phase diagrams of giant vesicles containing sphingomyelin.* Phys Rev Lett, 2005. **94**(14): p. 148101.
16. Veatch, S.L. and S.L. Keller, *Separation of liquid phases in giant vesicles of ternary mixtures of phospholipids and cholesterol.* Biophys J, 2003. **85**(5): p. 3074-83.

17. Holland, G.P., S.K. McIntyre, and T.M. Alam, *Distinguishing individual lipid headgroup mobility and phase transitions in raft-forming lipid mixtures with 31P MAS NMR.* Biophys J, 2006. **90**(11): p. 4248-60.
18. Simons, K. and G. van Meer, *Lipid sorting in epithelial cells.* Biochemistry, 1988. **27**(17): p. 6197-202.
19. van Meer, G. and K. Simons, *Lipid polarity and sorting in epithelial cells.* J Cell Biochem, 1988. **36**(1): p. 51-8.
20. Yu, J., D.A. Fischman, and T.L. Steck, *Selective solubilization of proteins and phospholipids from red blood cell membranes by nonionic detergents.* J Supramol Struct, 1973. **1**(3): p. 233-48.
21. Brown, D.A. and J.K. Rose, *Sorting of GPI-anchored proteins to glycolipid-enriched membrane subdomains during transport to the apical cell surface.* Cell, 1992. **68**(3): p. 533-44.
22. Schroeder, R., E. London, and D. Brown, *Interactions between saturated acyl chains confer detergent resistance on lipids and glycosylphosphatidylinositol (GPI)-anchored proteins: GPI-anchored proteins in liposomes and cells show similar behavior.* Proc Natl Acad Sci U S A, 1994. **91**(25): p. 12130-4.
23. Silvius, J.R., D. del Giudice, and M. Lafleur, *Cholesterol at different bilayer concentrations can promote or antagonize lateral segregation of phospholipids of differing acyl chain length.* Biochemistry, 1996. **35**(48): p. 15198-208.
24. Ahmed, S.N., D.A. Brown, and E. London, *On the origin of sphingolipid/ cholesterol-rich detergent-insoluble cell membranes: physiological concentrations of cholesterol and sphingolipid induce formation of a detergent-insoluble, liquid-ordered lipid phase in model membranes.* Biochemistry, 1997. **36**(36): p. 10944-53.
25. London, E., *How principles of domain formation in model membranes may explain ambiguities concerning lipid raft formation in cells.* Biochim Biophys Acta, 2005. **1746**(3): p. 203-20.
26. London, E., *Insights into lipid raft structure and formation from experiments in model membranes.* Curr Opin Struct Biol, 2002. **12**(4): p. 480-6.
27. de Almeida, R.F., L.M. Loura, and M. Prieto, *Membrane lipid domains and rafts: current applications of fluorescence lifetime spectroscopy and imaging.* Chem Phys Lipids, 2009. **157**(2): p. 61-77.
28. Loura, L.M., et al., *FRET analysis of domain formation and properties in complex membrane systems.* Biochim Biophys Acta, 2009. **1788**(1): p. 209-24.
29. Caffrey, M. and G.W. Feigenson, *Fluorescence quenching in model membranes. 3. Relationship between calcium adenosinetriphosphatase enzyme activity and the*

affinity of the protein for phosphatidylcholines with different acyl chain characteristics. Biochemistry, 1981. **20**(7): p. 1949-61.
30. Bakht, O. and E. London, *Detecting ordered domain formation (lipid rafts) in model membranes using Tempo.* Methods Mol Biol, 2007. **398**: p. 29-40.
31. Bacia, K., P. Schwille, and T. Kurzchalia, *Sterol structure determines the separation of phases and the curvature of the liquid-ordered phase in model membranes.* Proc Natl Acad Sci U S A, 2005. **102**(9): p. 3272-7.
32. Baumgart, T., et al., *Membrane elasticity in giant vesicles with fluid phase coexistence.* Biophys J, 2005. **89**(2): p. 1067-80.
33. Bakht, O., P. Pathak, and E. London, *Effect of the structure of lipids favoring disordered domain formation on the stability of cholesterol-containing ordered domains (lipid rafts): identification of multiple raft-stabilization mechanisms.* Biophys J, 2007. **93**(12): p. 4307-18.
34. Wassall, S.R., et al., *Order from disorder, corralling cholesterol with chaotic lipids. The role of polyunsaturated lipids in membrane raft formation.* Chem Phys Lipids, 2004. **132**(1): p. 79-88.
35. Megha, O. Bakht, and E. London, *Cholesterol precursors stabilize ordinary and ceramide-rich ordered lipid domains (lipid rafts) to different degrees. Implications for the Bloch hypothesis and sterol biosynthesis disorders.* J Biol Chem, 2006. **281**(31): p. 21903-13.
36. Wang, J., Megha, and E. London, *Relationship between sterol/steroid structure and participation in ordered lipid domains (lipid rafts): implications for lipid raft structure and function.* Biochemistry, 2004. **43**(4): p. 1010-8.
37. Xu, X., et al., *Effect of the structure of natural sterols and sphingolipids on the formation of ordered sphingolipid/sterol domains (rafts). Comparison of cholesterol to plant, fungal, and disease-associated sterols and comparison of sphingomyelin, cerebrosides, and ceramide.* J Biol Chem, 2001. **276**(36): p. 33540-6.
38. Xu, X. and E. London, *The effect of sterol structure on membrane lipid domains reveals how cholesterol can induce lipid domain formation.* Biochemistry, 2000. **39**(5): p. 843-9.
39. Huang, J. and G.W. Feigenson, *A microscopic interaction model of maximum solubility of cholesterol in lipid bilayers.* Biophys J, 1999. **76**(4): p. 2142-57.
40. Megha and E. London, *Ceramide selectively displaces cholesterol from ordered lipid domains (rafts): implications for lipid raft structure and function.* J Biol Chem, 2004. **279**(11): p. 9997-10004.

41. Megha, et al., *Effect of ceramide N-acyl chain and polar headgroup structure on the properties of ordered lipid domains (lipid rafts).* Biochim Biophys Acta, 2007. **1768**(9): p. 2205-12.
42. Yu, C., M. Alterman, and R.T. Dobrowsky, *Ceramide displaces cholesterol from lipid rafts and decreases the association of the cholesterol binding protein caveolin-1.* J Lipid Res, 2005. **46**(8): p. 1678-91.
43. Silva, L.C., et al., *Ceramide-domain formation and collapse in lipid rafts: membrane reorganization by an apoptotic lipid.* Biophys J, 2007. **92**(2): p. 502-16.
44. Chiantia, S., et al., *Role of ceramide in membrane protein organization investigated by combined AFM and FCS.* Biochim Biophys Acta, 2008. **1778**(5): p. 1356-64.
45. Chiantia, S., et al., *Effects of ceramide on liquid-ordered domains investigated by simultaneous AFM and FCS.* Biophys J, 2006. **90**(12): p. 4500-8.
46. Feigenson, G.W. and J.T. Buboltz, *Ternary phase diagram of dipalmitoyl-PC/ dilauroyl-PC/cholesterol: nanoscopic domain formation driven by cholesterol.* Biophys J, 2001. **80**(6): p. 2775-88.
47. Varma, R. and S. Mayor, *GPI-anchored proteins are organized in submicron domains at the cell surface.* Nature, 1998. **394**(6695): p. 798-801.
48. Kiessling, V., J.M. Crane, and L.K. Tamm, *Transbilayer effects of raft-like lipid domains in asymmetric planar bilayers measured by single molecule tracking.* Biophys J, 2006. **91**(9): p. 3313-26.
49. Wan, C., V. Kiessling, and L.K. Tamm, *Coupling of cholesterol-rich lipid phases in asymmetric bilayers.* Biochemistry, 2008. **47**(7): p. 2190-8.
50. Kiessling, V., C. Wan, and L.K. Tamm, *Domain coupling in asymmetric lipid bilayers.* Biochim Biophys Acta, 2009. **1788**(1): p. 64-71.
51. Cheng, H.T., Megha, and E. London, *Preparation and properties of asymmetric vesicles that mimic cell membranes: effect upon lipid raft formation and transmembrane helix orientation.* J Biol Chem, 2009. **284**(10): p. 6079-92.
52. Wolf, A.A., et al., *Ganglioside structure dictates signal transduction by cholera toxin and association with caveolae-like membrane domains in polarized epithelia.* J Cell Biol, 1998. **141**(4): p. 917-27.
53. Fujinaga, Y., et al., *Gangliosides that associate with lipid rafts mediate transport of cholera and related toxins from the plasma membrane to endoplasmic reticulm.* Mol Biol Cell, 2003. **14**(12): p. 4783-93.
54. Kirkham, M., et al., *Ultrastructural identification of uncoated caveolin-independent early endocytic vehicles.* J Cell Biol, 2005. **168**(3): p. 465-76.

55. Fujinaga, Y., *Transport of bacterial toxins into target cells: pathways followed by cholera toxin and botulinum progenitor toxin.* J Biochem, 2006. **140**(2): p. 155-60.
56. Lencer, W.I. and D. Saslowsky, *Raft trafficking of AB5 subunit bacterial toxins.* Biochim Biophys Acta, 2005. **1746**(3): p. 314-21.
57. London, E. and D.A. Brown, *Insolubility of lipids in triton X-100: physical origin and relationship to sphingolipid/cholesterol membrane domains (rafts).* Biochim Biophys Acta, 2000. **1508**(1-2): p. 182-95.
58. Heerklotz, H., *Interactions of surfactants with lipid membranes.* Q Rev Biophys, 2008. **41**(3-4): p. 205-64.
59. Brown, D.A., *Lipid rafts, detergent-resistant membranes, and raft targeting signals.* Physiology (Bethesda), 2006. **21**: p. 430-9.
60. Glebov, O.O. and B.J. Nichols, *Distribution of lipid raft markers in live cells.* Biochem Soc Trans, 2004. **32**(Pt 5): p. 673-5.
61. Kenworthy, A.K., et al., *Dynamics of putative raft-associated proteins at the cell surface.* J Cell Biol, 2004. **165**(5): p. 735-46.
62. Kenworthy, A.K., N. Petranova, and M. Edidin, *High-resolution FRET microscopy of cholera toxin B-subunit and GPI-anchored proteins in cell plasma membranes.* Mol Biol Cell, 2000. **11**(5): p. 1645-55.
63. Sharma, P., et al., *Nanoscale organization of multiple GPI-anchored proteins in living cell membranes.* Cell, 2004. **116**(4): p. 577-89.
64. Melkonian, K.A., et al., *Characterization of proteins in detergent-resistant membrane complexes from Madin-Darby canine kidney epithelial cells.* Biochemistry, 1995. **34**(49): p. 16161-70.
65. Fastenberg, M.E., et al., *Exclusion of a transmembrane-type peptide from ordered-lipid domains (rafts) detected by fluorescence quenching: extension of quenching analysis to account for the effects of domain size and domain boundaries.* Biochemistry, 2003. **42**(42): p. 12376-90.
66. Kenworthy, A.K., *Have we become overly reliant on lipid rafts? Talking Point on the involvement of lipid rafts in T-cell activation.* EMBO Rep, 2008. **9**(6): p. 531-5.
67. Bijlmakers, M.J., *Protein acylation and localization in T cell signaling (Review).* Mol Membr Biol, 2009. **26**(1): p. 93-103.
68. Shogomori, H., et al., *Palmitoylation and intracellular domain interactions both contribute to raft targeting of linker for activation of T cells.* J Biol Chem, 2005. **280**(19): p. 18931-42.
69. Parker, M.W. and S.C. Feil, *Pore-forming protein toxins: from structure to function.* Prog Biophys Mol Biol, 2005. **88**(1): p. 91-142.

70. Aroian, R. and F.G. van der Goot, *Pore-forming toxins and cellular non-immune defenses (CNIDs).* Curr Opin Microbiol, 2007. **10**(1): p. 57-61.
71. Voskoboinik, I., M.J. Smyth, and J.A. Trapani, *Perforin-mediated target-cell death and immune homeostasis.* Nat Rev Immunol, 2006. **6**(12): p. 940-52.
72. Rosado, C.J., et al., *The MACPF/CDC family of pore-forming toxins.* Cell Microbiol, 2008. **10**(9): p. 1765-74.
73. Giddings, K.S., A.E. Johnson, and R.K. Tweten, *Redefining cholesterol's role in the mechanism of the cholesterol-dependent cytolysins.* Proc Natl Acad Sci U S A, 2003. **100**(20): p. 11315-20.
74. Giddings, K.S., et al., *Human CD59 is a receptor for the cholesterol-dependent cytolysin intermedilysin.* Nat Struct Mol Biol, 2004. **11**(12): p. 1173-8.
75. Rossjohn, J., et al., *Structure of a cholesterol-binding, thiol-activated cytolysin and a model of its membrane form.* Cell, 1997. **89**(5): p. 685-92.
76. Rossjohn, J., et al., *Structures of perfringolysin O suggest a pathway for activation of cholesterol-dependent cytolysins.* J Mol Biol, 2007. **367**(5): p. 1227-36.
77. Heuck, A.P., et al., *Conformational Changes That Effect Oligomerization and Initiate Pore Formation Are Triggered throughout Perfringolysin O upon Binding to Cholesterol.* J Biol Chem, 2007. **282**(31): p. 22629-37.
78. Czajkowsky, D.M., et al., *Vertical collapse of a cytolysin prepore moves its transmembrane beta-hairpins to the membrane.* Embo J, 2004. **23**(16): p. 3206-15.
79. Soltani, C.E., et al., *Specific protein-membrane contacts are required for prepore and pore assembly by a cholesterol-dependent cytolysin.* J Biol Chem, 2007. **282**(21): p. 15709-16.
80. Polekhina, G., et al., *Insights into the action of the superfamily of cholesterol-dependent cytolysins from studies of intermedilysin.* Proc Natl Acad Sci U S A, 2005. **102**(3): p. 600-5.
81. Iwamoto, M., Y. Ohno-Iwashita, and S. Ando, *Role of the essential thiol group in the thiol-activated cytolysin from Clostridium perfringens.* Eur J Biochem, 1987. **167**(3): p. 425-30.
82. Soltani, C.E., et al., *Structural elements of the cholesterol-dependent cytolysins that are responsible for their cholesterol-sensitive membrane interactions.* Proc Natl Acad Sci U S A, 2007. **104**(51): p. 20226-31.
83. Gekara, N.O., et al., *The cholesterol-dependent cytolysin listeriolysin O aggregates rafts via oligomerization.* Cell Microbiol, 2005. **7**(9): p. 1345-56.

84. Shimada, Y., et al., *The C-terminal domain of perfringolysin O is an essential cholesterol-binding unit targeting to cholesterol-rich microdomains.* Eur J Biochem, 2002. **269**(24): p. 6195-203.
85. Ohno-Iwashita, Y., et al., *Perfringolysin O, a cholesterol-binding cytolysin, as a probe for lipid rafts.* Anaerobe, 2004. **10**(2): p. 125-34.
86. Waheed, A.A., et al., *Selective binding of perfringolysin O derivative to cholesterol-rich membrane microdomains (rafts).* Proc Natl Acad Sci U S A, 2001. **98**(9): p. 4926-31.
87. Shepard, L.A., et al., *The mechanism of pore assembly for a cholesterol-dependent cytolysin: formation of a large prepore complex precedes the insertion of the transmembrane beta-hairpins.* Biochemistry, 2000. **39**(33): p. 10284-93.
88. Nakamura, M., et al., *Interaction of theta-toxin (perfringolysin O), a cholesterol-binding cytolysin, with liposomal membranes: change in the aromatic side chains upon binding and insertion.* Biochemistry, 1995. **34**(19): p. 6513-20.
89. Tweten, R.K., M.W. Parker, and A.E. Johnson, *The cholesterol-dependent cytolysins.* Curr Top Microbiol Immunol, 2001. **257**: p. 15-33.
90. Petit, L., M. Gibert, and M.R. Popoff, *Clostridium perfringens: toxinotype and genotype.* Trends Microbiol, 1999. **7**(3): p. 104-10.
91. O'Brien, D.K. and S.B. Melville, *Effects of Clostridium perfringens alpha-toxin (PLC) and perfringolysin O (PFO) on cytotoxicity to macrophages, on escape from the phagosomes of macrophages, and on persistence of C. perfringens in host tissues.* Infect Immun, 2004. **72**(9): p. 5204-15.
92. Johnson, M.K., C. Geoffroy, and J.E. Alouf, *Binding of cholesterol by sulfhydryl-activated cytolysins.* Infect Immun, 1980. **27**(1): p. 97-101.
93. Ramachandran, R., R.K. Tweten, and A.E. Johnson, *The domains of a cholesterol-dependent cytolysin undergo a major FRET-detected rearrangement during pore formation.* Proc Natl Acad Sci U S A, 2005. **102**(20): p. 7139-44.
94. Gilbert, R.J., et al., *Two structural transitions in membrane pore formation by pneumolysin, the pore-forming toxin of Streptococcus pneumoniae.* Cell, 1999. **97**(5): p. 647-55.
95. Ramachandran, R., et al., *Structural insights into the membrane-anchoring mechanism of a cholesterol-dependent cytolysin.* Nat Struct Biol, 2002. **9**(11): p. 823-7.
96. Geoffroy, C. and J.E. Alouf, *Selective purification by thiol-disulfide interchange chromatography of alveolysin, a sulfhydryl-activated toxin of Bacillus alvei. Toxin properties and interaction with cholesterol and liposomes.* J Biol Chem, 1983. **258**(16): p. 9968-72.

97. Simons, K. and W.L. Vaz, *Model systems, lipid rafts, and cell membranes.* Annu Rev Biophys Biomol Struct, 2004. **33**: p. 269-95.
98. Rebolj, K., et al., *Steroid structural requirements for interaction of ostreolysin, a lipid-raft binding cytolysin, with lipid monolayers and bilayers.* Biochim Biophys Acta, 2006. **1758**(10): p. 1662-70.
99. Alouf, J.E., et al., *Surface properties of bacterial sulfhydryl-activated cytolytic toxins. Interaction with monomolecular films of phosphatidylcholine and various sterols.* Eur J Biochem, 1984. **141**(1): p. 205-10.
100. Prigent, D. and J.E. Alouf, *Interaction of steptolysin O with sterols.* Biochim Biophys Acta, 1976. **443**(2): p. 288-300.
101. Watson, K.C. and E.J. Kerr, *Sterol structural requirements for inhibition of streptolysin O activity.* Biochem J, 1974. **140**(1): p. 95-8.
102. Bavdek, A., et al., *Sterol and pH interdependence in the binding, oligomerization, and pore formation of Listeriolysin O.* Biochemistry, 2007. **46**(14): p. 4425-37.
103. Pinkney, M., E. Beachey, and M. Kehoe, *The thiol-activated toxin streptolysin O does not require a thiol group for cytolytic activity.* Infect Immun, 1989. **57**(8): p. 2553-8.
104. Chung, L.A. and E. London, *Interaction of diphtheria toxin with model membranes.* Biochemistry, 1988. **27**(4): p. 1245-53.
105. Emans, N., J. Biwersi, and A.S. Verkman, *Imaging of endosome fusion in BHK fibroblasts based on a novel fluorimetric avidin-biotin binding assay.* Biophys J, 1995. **69**(2): p. 716-28.
106. Nicol, F., S. Nir, and F.C. Szoka, Jr., *Orientation of the pore-forming peptide GALA in POPC vesicles determined by a BODIPY-avidin/biotin binding assay.* Biophys J, 1999. **76**(4): p. 2121-41.
107. Nir, S., F. Nicol, and F.C. Szoka, Jr., *Surface aggregation and membrane penetration by peptides: relation to pore formation and fusion.* Mol Membr Biol, 1999. **16**(1): p. 95-101.
108. Hotze, E.M., et al., *Monomer-monomer interactions drive the prepore to pore conversion of a beta-barrel-forming cholesterol-dependent cytolysin.* J Biol Chem, 2002. **277**(13): p. 11597-605.
109. Geisow, M.J., P. D'Arcy Hart, and M.R. Young, *Temporal changes of lysosome and phagosome pH during phagolysosome formation in macrophages: studies by fluorescence spectroscopy.* J Cell Biol, 1981. **89**(3): p. 645-52.
110. Portnoy, D.A., et al., *Capacity of listeriolysin O, streptolysin O, and perfringolysin O to mediate growth of Bacillus subtilis within mammalian cells.* Infect Immun, 1992. **60**(7): p. 2710-7.

111. Geoffroy, C., et al., *Purification, characterization, and toxicity of the sulfhydryl-activated hemolysin listeriolysin O from Listeria monocytogenes.* Infect Immun, 1987. **55**(7): p. 1641-6.
112. London, E., *How bacterial protein toxins enter cells; the role of partial unfolding in membrane translocation.* Mol Microbiol, 1992. **6**(22): p. 3277-82.
113. Wang, J., M.P. Rosconi, and E. London, *Topography of the hydrophilic helices of membrane-inserted diphtheria toxin T domain: TH1-TH3 as a hydrophilic tether.* Biochemistry, 2006. **45**(26): p. 8124-34.
114. Zhao, J.M. and E. London, *Similarity of the conformation of diphtheria toxin at high temperature to that in the membrane-penetrating low-pH state.* Proc Natl Acad Sci U S A, 1986. **83**(7): p. 2002-6.
115. Bakht, O., Pathak, P., and London, E. , *Effect of the Acyl Chain and Headgroup Structure of Lipids Favoring Disordered Domain Formation on the Stability of Cholesterol-Containing Ordered Domains (Lipid Rafts): Identification of Multiple Raft-Stabilization Mechanisms by Low-Tm Lipids.* Biophys. J, 2007. ***in press***.
116. Zitzer, A., et al., *Coupling of cholesterol and cone-shaped lipids in bilayers augments membrane permeabilization by the cholesterol-specific toxins streptolysin O and Vibrio cholerae cytolysin.* J Biol Chem, 2001. **276**(18): p. 14628-33.
117. Ohno-Iwashita, Y., et al., *Effect of lipidic factors on membrane cholesterol topology--mode of binding of theta-toxin to cholesterol in liposomes.* Biochim Biophys Acta, 1992. **1109**(1): p. 81-90.
118. Beattie, M.E., et al., *Sterol structure determines miscibility versus melting transitions in lipid vesicles.* Biophys J, 2005. **89**(3): p. 1760-8.
119. Hammond, A.T., et al., *Crosslinking a lipid raft component triggers liquid ordered-liquid disordered phase separation in model plasma membranes.* Proc Natl Acad Sci U S A, 2005. **102**(18): p. 6320-5.
120. Niu, S.L. and B.J. Litman, *Determination of membrane cholesterol partition coefficient using a lipid vesicle-cyclodextrin binary system: effect of phospholipid acyl chain unsaturation and headgroup composition.* Biophys J, 2002. **83**(6): p. 3408-15.
121. Leventis, R. and J.R. Silvius, *Use of cyclodextrins to monitor transbilayer movement and differential lipid affinities of cholesterol.* Biophys J, 2001. **81**(4): p. 2257-67.
122. Gekara, N.O. and S. Weiss, *Lipid rafts clustering and signalling by listeriolysin O.* Biochem Soc Trans, 2004. **32**(Pt 5): p. 712-4.
123. Flanagan, J.J., et al., *Cholesterol Exposure at the Membrane Surface Is Necessary and Sufficient to Trigger Perfringolysin O Binding.* Biochemistry, 2009.

124. Nelson, L.D., A.E. Johnson, and E. London, *How interaction of perfringolysin O with membranes is controlled by sterol structure, lipid structure, and physiological low pH: insights into the origin of perfringolysin O-lipid raft interaction.* J Biol Chem, 2008. **283**(8): p. 4632-42.
125. Perrin, F., C.R. Hebd. Seances Acad. Sci., 1924(178): p. 1978.
126. Chattopadhyay, A. and E. London, *Parallax Method for Direct Measurement of Membrane Penetration Depth Utilizing Fluorescence Quenching by Spin-Labeled Phospholipids.* Biochemistry, 1987. **26**: p. 39-45.
127. Beck, A., D. Heissler, and G. Duportail, *Influence of the length of the spacer on the partitioning properties of amphiphilic fluorescent membrane probes.* Chem Phys Lipids, 1993. **66**(1-2): p. 135-42.
128. Bjorkqvist, Y.J., et al., *Domain formation and stability in complex lipid bilayers as reported by cholestatrienol.* Biophys J, 2005. **88**(6): p. 4054-63.
129. Nybond, S., et al., *Acyl chain length affects ceramide action on sterol/ sphingomyelin-rich domains.* Biochim Biophys Acta, 2005. **1718**(1-2): p. 61-6.
130. Alanko, S.M., et al., *Displacement of sterols from sterol/sphingomyelin domains in fluid bilayer membranes by competing molecules.* Biochim Biophys Acta, 2005. **1715**(2): p. 111-21.
131. Silvius, J.R., *Role of cholesterol in lipid raft formation: lessons from lipid model systems.* Biochim Biophys Acta, 2003. **1610**(2): p. 174-83.
132. Hess, S.T., et al., *Shape analysis of giant vesicles with fluid phase coexistence by laser scanning microscopy to determine curvature, bending elasticity, and line tension.* Methods Mol Biol, 2007. **400**: p. 367-87.
133. Kahya, N., *Targeting membrane proteins to liquid-ordered phases: molecular self-organization explored by fluorescence correlation spectroscopy.* Chem Phys Lipids, 2006. **141**(1-2): p. 158-68.

Appendix

Structures of sterols used in Chapter 3.